Elsevier Editorial System(tm) for Lithos
Manuscript Draft

Manuscript Number: LITHOS6453R2

Title: Coexistence of alkaline-carbonatite complexes and high-MgO CFB in the Paranà-Etendeka province: Insights on plume-lithosphere interactions in the Gondwana realm

Article Type: Review Article

Keywords: Paranà-Etendeka; high-MgO CFB; alkaline-carbonatite complexes; plume-lithosphere interaction

Corresponding Author: Professor Luigi Beccaluva, Full Professor

Corresponding Author's Institution: Università di Ferrara

First Author: Claudio Natali, PhD

Order of Authors: Claudio Natali, PhD; Luigi Beccaluva, Full Professor; Gianluca Bianchini, Prof.; Franca Siena, Prof.

Abstract: A careful review of petrological and geochemical data on the Paranà-Etendeka igneous province is reported, with particular attention being devoted to the relationships between high-MgO CFB (tholeiitic basalts-picrites) and nearly coeval alkaline-carbonatite complexes linked to the same extensional tectonics on a regional scale. At 135-130 Ma, the tectonomagmatic activity was focused in Etendeka, the centre of the restored province, and characterised by an exclusive occurrence of the hottest and deepest high-MgO CFB (potential temperature Tp up to 1590°C and pressure up to 5 GPa) possessing the same Sr-Nd-Pb isotopic composition of the "Gough" geochemical component, a marker of the initial Tristan plume activity. Etendeka high-MgO CFB thus represent the most genuine proxies of sublithospheric melts generated at the plume axis and are relatively unaffected by lithospheric contamination. Nearly coeval (133-128 Ma) alkaline-carbonatite complexes cluster around the extensional structures of the Ponta Grossa Arch (e.g., Jacupiranga and Juquia in Brazil) and the Damara Belt (e.g., Erongo, Okurusu, Okenyenya and Paresis in Namibia), both of which intersect the early track of the south Atlantic opening. Compared to high-MgO CFB, alkaline magmas display distinctive isotopic signatures and an incompatible element distribution consistent with their generation from lithospheric mantle sources, which were variably metasomatised (veined?) by amphibole and phlogopite. Metasomes of alkaline mantle sources have a HIMU affinity and are dominated by amphibole in Namibia, whereas they display EM tendency and a more relevant role of phlogopite in Brazil, which implies important lithospheric differences at a regional scale. The tectonomagmatic features of Paranà-Etendeka -also shared by other Gondwana LIPs, such as Deccan and Karoo- can be reconciled by a generalized model where a hot plume impinging on a relatively thick lithosphere caused, in the axial zone, the contemporaneous generation and rise of high-MgO CFB and alkaline magmas from distinct asthenospheric and lithospheric mantle sources, respectively. In the asthenosphere, the volatile-poor solidus was crossed under an adiabatic thermal regime, mostly in the range of 4 to 5 GPa and Tp 1500 to 1600°C with the development of high-MgO CFB. In the overlying metasomatised lithosphere, the plume effects caused a

perturbation of the conductive thermal regime and a crossing of volatile-rich solidus (mostly P 2-3 GPa, Tp 1300-1400°C) with the generation of alkaline melts from the most fusible (hydrated and carbonated) mantle domains.

Dear Editor

Thank you for your rapid decision and for the final corrections that have been promptly included in the manuscript.

Kind Regards,

Luigi Beccaluva and Co-authors.

Abstract

A careful review of petrological and geochemical data on the Paranà-Etendeka igneous province is reported, with particular attention being devoted to the relationships between high-MgO CFB (tholeiitic basalts-picrites) and nearly coeval alkaline-carbonatite complexes linked to the same extensional tectonics on a regional scale. At 135-130 Ma, the tectonomagmatic activity was focused in Etendeka, the centre of the restored province, and characterised by an exclusive occurrence of the hottest and deepest high-MgO CFB (potential temperature T_p up to 1590°C and pressure up to 5 GPa) possessing the same Sr-Nd-Pb isotopic composition of the "Gough" geochemical component, a marker of the initial Tristan plume activity. Etendeka high-MgO CFB thus represent the most genuine proxies of sublithospheric melts generated at the plume axis and are relatively unaffected by lithospheric contamination. Nearly coeval (133-128 Ma) alkaline-carbonatite complexes cluster around the extensional structures of the Ponta Grossa Arch (e.g., Jacupiranga and Juquia in Brazil) and the Damara Belt (e.g., Erongo, Okurusu, Okenyenya and Paresis in Namibia), both of which intersect the early track of the south Atlantic opening. Compared to high-MgO CFB, alkaline magmas display distinctive isotopic signatures and an incompatible element distribution consistent with their generation from lithospheric mantle sources, which were variably metasomatised (veined?) by amphibole and phlogopite. Metasomes of alkaline mantle sources have a HIMU affinity and are dominated by amphibole in Namibia, whereas they display EM tendency and a more relevant role of phlogopite in Brazil, which implies important lithospheric differences at a regional scale. The tectonomagmatic features of Paranà-Etendeka –also shared by other Gondwana LIPs, such as Deccan and Karoo– can be reconciled by a generalized model where a hot plume impinging on a relatively thick lithosphere caused, in the axial zone, the contemporaneous generation and rise of high-MgO CFB and alkaline magmas from distinct asthenospheric and lithospheric mantle sources, respectively. In the asthenosphere, the volatile-poor solidus was crossed under an adiabatic thermal regime, mostly in the range of 4 to 5 GPa and T_p 1500 to 1600°C with the development of high-MgO CFB. In the overlying metasomatised lithosphere, the plume

effects caused a perturbation of the conductive thermal regime and a crossing of volatile-rich solidus (mostly P 2-3 GPa, T_p 1300-1400°C) with the generation of alkaline melts from the most fusible (hydrated and carbonated) mantle domains.

Graphical Abstract (for review)

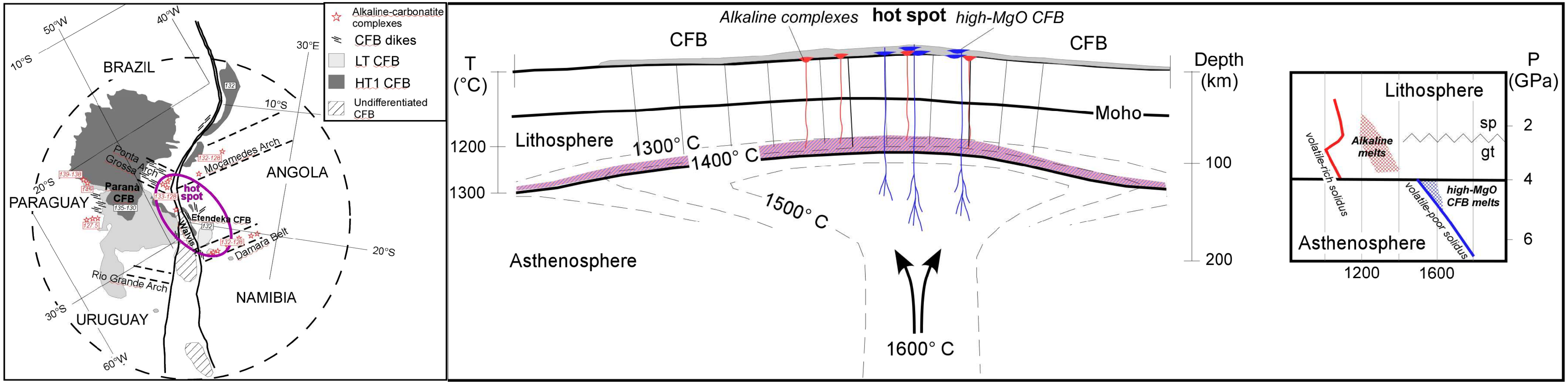

*Highlights (for review)

Research Highlights:

- High-MgO CFB and alkaline-carbonatite complexes coexist at the centre of Paranà-Etendeka LIP
- The two magma types are generated under distinct P-T-X conditions at the plume axial zone
- Similar tectonomagmatic occurrences are characteristic of other Gondwana LIPs
- High-MgO CFB magmas derived from plume-related sublithospheric mantle sources
- Alkaline magmas derived from metasomatized sources in the overlying lithosphere

Coexistence of alkaline-carbonatite complexes and high-MgO CFB in the Paranà-Etendeka province: Insights on plume-lithosphere interactions in the Gondwana realm

Claudio Natali, Luigi Beccaluva*, Gianluca Bianchini, Franca Siena

Department of Physics and Earth Sciences, University of Ferrara, via Saragat 1, 44121 Ferrara - Italy

***Corresponding author**: bcc@unife.it

Abstract

A careful review of petrological and geochemical data on the Paranà-Etendeka igneous province is reported, with particular attention being devoted to the relationships between high-MgO CFB (tholeiitic basalts-picrites) and nearly coeval alkaline-carbonatite complexes linked to the same extensional tectonics on a regional scale. At 135-130 Ma, the tectonomagmatic activity was focused in Etendeka, the centre of the restored province, and characterised by an exclusive occurrence of the hottest and deepest high-MgO CFB (potential temperature T_p up to 1590°C and pressure up to 5 GPa) possessing the same Sr-Nd-Pb isotopic composition of the "Gough" geochemical component, a marker of the initial Tristan plume activity. Etendeka high-MgO CFB thus represent the most genuine proxies of sublithospheric melts generated at the plume axis and are relatively unaffected by lithospheric contamination. Nearly coeval (133-128 Ma) alkaline-carbonatite complexes cluster around the extensional structures of the Ponta Grossa Arch (e.g., Jacupiranga and Juquia in Brazil) and the Damara Belt (e.g., Erongo, Okurusu, Okenyenya and Paresis in Namibia), both of which intersect the early track of the south Atlantic opening. Compared to high-MgO CFB, alkaline magmas display distinctive isotopic signatures and an incompatible element distribution consistent with their generation from lithospheric mantle sources, which were variably metasomatised (veined?) by amphibole and phlogopite. Metasomes of alkaline mantle sources have a HIMU affinity and are dominated by amphibole in Namibia, whereas they display EM1 tendency and a more relevant role of phlogopite in Brazil, which implies important lithospheric differences at a regional scale. The tectonomagmatic features of Paranà-Etendeka –also shared by other Gondwana LIPs, such as Deccan and Karoo– can be reconciled by a generalized model where a hot plume impinging on a relatively thick lithosphere caused, in the axial zone, the contemporaneous generation and rise of high-MgO CFB and alkaline magmas from distinct asthenospheric and lithospheric mantle sources, respectively. In the asthenosphere, the volatile-poor solidus was crossed under an adiabatic thermal regime, mostly in the range of 4 to 5 GPa and T_p 1500 to 1600°C with the development of high-MgO CFB. In the overlying metasomatised lithosphere, the plume effects caused a perturbation of the conductive thermal regime and a crossing of volatile-rich solidus (mostly P 2-3 GPa, T_p 1300-1400°C) with the generation of alkaline melts from the most fusible (hydrated and carbonated) mantle domains.

1. Introduction

In the last decades, several authors have drawn attention to the close spatial-temporal relationships between alkaline-carbonatite complexes and Continental Flood Basalts (CFB) in many Large Igneous Provinces (LIP), giving rise to a longstanding debate on the role of lithosphere and plume/asthenosphere components of their respective magma sources (Ellam and Cox, 1991; Bell, 2001; Gibson et al., 2006; Campbell, 2007; Ernst and Bell, 2010; Safonova and Santosh, 2014; Pirajino, 2015). Specifically, in the Gondwana realm, alkaline-carbonatite complexes appear to be closely related to high-MgO picrite-basalt rocks at the intersection of rift structures characterising the inner part of plume-related CFB provinces, such as Karoo and Deccan (Natali et al., 2017) and, particularly, Paranà-Etendeka, where these rock associations are well-documented (Comin-

Chiaramonti et al., 2011; Gomes et al., 2011). For the latter province, petrogenetic investigations have relevant implications considering the debated origin of the Paranà-Etendeka, which is either related to the Early Cretaceous activation of the proto-Tristan plume (Cordani et al., 1980; White and McKenzie, 1989; 1995; Bizzi et al., 1995; Gibson et al., 1995; 2006; Thompson et al., 2001; Campbell, 2001; Tuff et al., 2005; Campbell and Davies, 2006) or to passive rifting events that mainly involved melting of the lithosphere (Peate et al., 1999; Hawkesworth et al., 2000; Ernesto et al., 2002; Iacumin et al., 2003; Guarino et al., 2013; Rocha-Junior et al., 2013).

Therefore, the integrated study of nearly coeval high-MgO CFB and alkaline igneous rocks from this province represents a very convenient case study to investigate their genetic relationships, including P-T conditions, source compositions and melting degree within a coherent tectonomagmatic framework. For this purpose, more than three thousand analyses from the literature, including major/trace and Sr-Nd-Pb isotopic data have been revisited, emphasising the petrological and geochemical characteristics of CFB and the nearly coeval alkaline-carbonatite complexes. In addition, the review includes the analogous occurrences from Deccan and Karoo with the aim of evaluating, within a homogeneous scheme, whether these recurrent igneous associations of west-central Gondwana may be attributed to a common tectono-magmatic scenario.

2. Methods

Bulk rock chemical analyses of CFB and associated alkaline-carbonatite complexes from the three investigated provinces were retrieved by the GEOROC database. For Paranà-Etendeka, CFB samples were reclassified as Low-Ti (LT) and High-Ti (HT1) suites, discriminating samples on the basis of Ti, Fe, Nb and Ce, as recently proposed by Natali et al. (2016; 2017) for the Deccan and Karoo provinces. Major element compositions of the investigated igneous associations are discussed and compared with the experimental petrology data in order to constrain phase equilibria and conditions of magma generation (Walter, 1998; Green and Fallon, 2005; Gudfinnsson and

Presnall, 2005; Dasgupta et al., 2007; Pilet et al., 2008). Reconstruction of primary magmas and the relative thermobarometric conditions were estimated according to PRIMELT3MEGA (Herzberg and Asimow, 2015), FRACTIONATEPT (Lee et al., 2009) and MANTLEPT (Putirka, 2016) using major element compositions, whereas incompatible trace elements were used to constrain source enrichment and the degree of melting (Pilet et al., 2011). Moreover, the available Sr-Nd-Pb isotopic data were taken into consideration to constrain the nature of magma sources in terms of mantle components (Zindler and Hart, 1986; Hofmann, 1997; Stracke et al., 2012).

3. High-MgO CFB and associated alkaline-carbonatite complexes in west-central Gondwana

3.1 Paranà-Etendeka igneous Province

The Paranà-Etendeka CFB province of the south American and southwest African margins mostly consists of LT and HT1 basalts, locally topped by rhyolitic volcanic rocks (Bellieni et al., 1986; Piccirillo and Melfi, 1988; Piccirillo et al., 1989; 1990). The chronology of CFB spans from 139 to 128 Ma, with the oldest recorded ages occurring in some basalts of western Paranà. The main magmatic phases are in the range of 135-130 Ma (Stewart et al., 1996; Renne et al., 1996a; 1996b; Gibson et al., 2006; Thiede and Vasconcelos, 2010; Janasi et al., 2011; Pinto et al., 2011).

Geochemical data reviewed in this work are used for the paleogeographic reconstruction of the Paranà-Etendeka province reported in Fig. 1. CFB are classified in LT (TiO_2 0.5-2.5 wt%) and HT1 (TiO_2 2.0-4.5 wt%) suites, as shown in Fig. 2. In the Etendeka region, both suites include high-MgO (> 10 wt%) basaltic and picritic rocks typically represented by HT1 Doros picrites, olivine-rich gabbroic intrusives and LT Horingbaai dikes (Thompson et al., 2001; Jennings et al., 2017; Owen-Smith et al., 2017). The significant systematic increase of incompatible elements (such as Nb and Ce) from LT to HT1 at comparable MgO values is illustrated in Fig. 2. Chondrite-Normalized Rare Earth Element (REE) patterns show a significant increase in the La_N/Yb_N ratio from LT to

HT1 (4.0-4.7 in LT, 7.0-8.5 in HT1; Fig. 3), indicating a systematic enrichment of incompatible elements and/or a lower melting degree of HT mantle sources. In the petrogenetic grid of Fig. 4, the two suites show distinct FeO enrichment at comparable MgO, particularly for the least fractionated lavas, suggesting mantle sources with different iron content. Representative differentiation trends modelled for the two suites (PETROLOG v.3, Danyushevsky and Pletchov, 2011) show that they are both characterised by the early fractionation of olivine (Ol), followed by clinopyroxene (Cpx) for HT1, and plagioclase (Pl) and Cpx for LT, which are consistent with the phenocryst assemblages observed in the rocks.

The reconstruction of primary magmas and their potential temperature (T_p) have been performed through the accumulated fractional melting algorithm PRIMELT3MEGA (Herzberg and Asimow, 2015), assuming the anhydrous lherzolite KR4003 (Walter, 1998) as a mantle source having mg# of 0.90, which is suitable for tholeiitic magmas. The calculated primary melts have MgO 21.2 wt%, FeO 11.1 wt%, mantle potential temperature (T_p) ~ 1590°C for HT1, and MgO 18.1 wt%, FeO 9.6 wt%, T_p ~ 1520°C for LT. Phase equilibria constraints and the application of geobarometers by Herzberg et al. (2007) and Guddfinnson and Presnall (2005) suggest that the generation of these primary melts occurred at ~ 5 GPa for HT1 and 3-4 GPa for LT (Supplementary Table 1). Compared to the above thermobarometric estimates, T_p obtained by the model of Lee et al. (2009) show a good agreement, and T_p by the model of Putirka (2016) are 70-80°C higher. Conversely, the pressures obtained by Lee et al. (2009) and Putirka (2016) are always underestimated with respect to those of Herzberg et al. (2007) and Guddfinnson and Presnall (2005; Supplementary Table 1). As shown by the Primitive Mantle (PM) incompatible element distribution (Fig. 5), the HT1 and LT primary magmas could be formed by 9% and 22% melting, respectively, from a mixed mantle source composed by 97% PM and 3% eclogite (recorded as xenoliths from Angolan kimberlites; Shervais et al., 1988).

The most representative alkaline complexes coeval (133-128 Ma) with CFB occur in the elliptical area depicted in Fig. 1, which corresponds to the centre of the restored Paranà-Etendeka province. In this area, several extensional lineaments converge towards the Walvis Ridge and the early track of the South Atlantic opening. On the south American side of the province, these complexes are represented by Juquia, Jacupiranga and Anitapolis, located in the Ponta Grossa Arch and along the Brazilian coast (Beccaluva et al., 1992; 2017; Gomes et al., 2011 and references therein). In the south-western African margin, alkaline and alkaline-carbonatite complexes are widespread in the Namibian Damara Belt (e.g., Erongo, Paresis, Okenyenya and Okurusu; Comin-Chiaramonti et al., 2011 and references therein) and in the Angolan Moçamedes Arch (e.g., Chivira-Bonga; Coltorti et al., 1993; Alberti et al. 1999).

The magmatic associations of alkaline complexes from both south American and African margins consist of mafic lithologies -such as alkali basalts, basanites/tephrites, nephelinites, and ankaratrites- or their plutonic counterpart, coupled with ultramafic cumulates, nepheline-syenites and carbonatites (Beccaluva et al., 1992; 2017; Morbidelli et al., 1995; Le Roex and Lanyon, 1998; Trumbull et al., 2003; Comin-Chiaramonti and Gomes, 2005; Ruberti et al., 2005; Gibson et al., 2006; Gomes et al., 2011; Azzone et al., 2013). All of these lithologies are silica-undersaturated with variable amounts of nepheline and the ubiquitous presence of hydrous phases, such as amphibole and/or phlogopite. The latter is the dominant hydrous phase in the Brazilian alkaline complexes, typically showing a more potassic character with respect to those from Namibia and Angola (Fig. 6). Accordingly, the PM-normalized incompatible element patterns of Fig. 7 show that the African alkaline magmas, unlike those from Brazil, are characterised by the presence of a significant negative K anomaly. As demonstrated by experimental petrology, this indicates a major role of amphibole with respect to phlogopite in mantle sources and a consequent K deficiency in the generated melts (K< 20000 ppm; Späth et al., 2001; Rooney et al., 2017). Therefore, for a comparable alkali/silica ratio, the potassic or sodic affinity of alkaline magmas depends on the relative phlogopite/amphibole proportion in their mantle sources. Generally, the significant presence of hydrous (and carbonated) phases is a necessary requirement in the genesis of alkaline melts, as invariably indicated by experimental petrology, either from 1) homogeneously metasomatised or 2) variably veined mantle sources. In the first case, experimental results (Green and Fallon, 2005; Gudfinnsson and Presnall, 2005; Dasgupta et al., 2007) show that alkaline magmas could be generated by decreasing the degree of partial melting (< 10% alkali basalts and basanites; < 5% nephelinites, melilitites and carbonatites) of hydrated and/or carbonated fertile lherzolite at increasing pressure from ~ 2 to 3.5 GPa within the lithosphere (Morris and Pasteris, 1987; Nielson and Wilshire, 1993). In the second case, alkaline basic melts (e.g., basanites, nephelinites) have been obtained by melting experiments on natural amphibole-rich veined lherzolites at 1.5 GPa (Pilet et al., 2011).

From the above, the modelling of alkaline melts has to include the effect of metasomatism, which decreases the mg# of the inferred source with respect to that of the unmetasomatised mantle. In fact, olivine composition in alkaline magmas is generally $\leq Fo_{88}$ (Harris et al., 1999; Coltorti et al., 1993; Beccaluva et al., 1992; 2017; Trumbull et al., 2003), a value that is significantly lower than that recorded in CFB (Fo up to 89-90; Beccaluva et al., 2009; Natali et al., 2016; 2017; Thompson and Gibson 2000), conforming to a source composition that does not exceed mg# 0.88. Accordingly, the Paranà-Etendeka alkaline primary magmas and the related P-T estimates have been modelled using the algorithms of Putirka (2016), which allows taking into proper account the effect of metasomatism. The results, which are reported in Supplementary Table 1, indicate that the investigated alkaline magmas are compatible with generation in the P range 1.8-2.0 GPa and T_p 1300-1360°C, by melting of a mantle source having mg# 0.87. Notably, these thermobarometric conditions approach those recorded by amphibole-bearing peridotite xenoliths from the Damara Belt lithosphere (Baumgartner et al., 2000; Le Roex and Class, 2014). As reported in Fig. 8, the incompatible element distribution of the Paranà-Etendeka alkaline magmas are satisfactorily reproduced assuming mantle sources variably enriched by metasomatic veins, as proposed by Pilet et al. (2008; 2011). The melting model of the African alkaline magmas indicates a best fit calculation either by a low melting degree (F ~ 2%) of a PM source hybridized by 20% amphibole-rich metasomatic veins or by a higher melting degree (F ~ 10%) of highly veined (40%) PM source

(Fig. 8a). Conversely, the more potassic character of alkaline melts from south America necessarily implies a significant presence of phlogopite, in addition to amphibole, in their mantle sources. In this case, best fit can be obtained either by F ~ 2% of a PM source hybridized by 40% amphibole-phlogopite veins, or by F ~ 8% of a PM source dominated by the amphibole-phlogopite metasome (90%, Fig. 8b). It is important to note that conceptually, in these models the metasomatising veins include variable proportions of cumulate hydrous minerals and residual liquids that could also be carbonated (Pilet et al., 2011). As recently observed in various volcanic provinces, this phenomenon conforms to the wide variability of lithospheric mantle sources, in terms of extent and composition of metasomatism, configuration of the lowered solidus and melting degrees (Jung et al., 2011; Rooney et al., 2017). Noteworthy, by a purely geochemical standpoint, the incompatible element distribution could also be approached by < 1% melting of an unmetasomatised (volatile-poor) mantle source, but this possibility is strongly discounted due to the ubiquitous evidence that alkaline magmas are significantly hydrated and carbonated.

The distribution of Sr-Nd-Pb isotopes for Paranà-Etendeka CFB and associated alkaline complexes is reported in Fig. 9. Taken as a whole, the two magmatic associations show distinct isotopic signatures that imply significant differences in their mantle sources. In particular, most high-MgO CFB from Etendeka (LT and HT1 picrites and some basalts) cluster in the upper left of the εNd-$^{87}Sr/^{86}Sr_{(i)}$ diagram covering a restricted isotopic range (εNd 9.1-0.5 and $^{87}Sr/^{86}Sr_{(i)}$ 0.70326-0.70513). As observed by other authors (Thompson et al., 2001; Hoernle et al., 2015; Owen-Smith et al., 2017) this isotopic signature is attributable to uncontaminated, sublithospheric mantle components. Conversely, all of the Paranà and the remaining Etendeka CFB (MgO 9-5 wt%) extend in the lower right quadrant towards low εNd (down to -10) and extremely high $^{87}Sr/^{86}Sr_{(i)}$ (up to 0.7142) values, reflecting the variable involvement of lithospheric mantle components and/or variable continental crust contamination at progressive differentiation. In particular, HT1 from Paranà display a relatively restricted isotopic range ($^{87}Sr/^{86}Sr_{(i)}$ 0.70495-0.70620 and εNd from -1.27 to -4.32) that could be related to a significant role of lithospheric components in their mantle sources, whereas the wide $^{87}Sr/^{86}Sr_{(i)}$ variation recorded in LT certainly reflects continental crust contamination. The Pb isotopic composition of the entire CFB population ranges between $^{207}Pb/^{204}Pb$ 15.4-15.8 and $^{206}Pb/^{204}Pb$ 17.1-19.7, with the abovementioned high-MgO Etendeka CFB plotting in the middle of the distribution. On the whole, the Sr-Nd-Pb isotope distributions of uncontaminated CFB from Etendeka shows a good agreement with the "Gough" component, which has been recently identified as the marker of the initial (proto-Tristan) plume activity since 133-132 Ma (Hoernle et al., 2015). In diagrams of Fig. 9 the Paranà-Etendeka alkaline complexes show distinct isotopic compositions that plausibly reflect a derivation from independent and different mantle sources: the Brazilian complexes extend from near FOZO (Prevalent mantle) to EM1 (εNd from +4.5 to -7.8, $^{87}Sr/^{86}Sr_{(i)}$ 0.70410-0.70632, $^{206}Pb/^{204}Pb$ 17.1-18.0), whereas those from Namibia and Angola display affinity with the HIMU component (εNd from +5.0 to -1.8, $^{87}Sr/^{86}Sr_{(i)}$ 0.70375-0.70487, $^{206}Pb/^{204}Pb$ 18.2-19.7). These different isotopic signatures appear to be correlated with the potassic *vs* sodic affinity, testifying for a different history of metasomatic enrichment in the lithospheric mantle of the south American and African margins.

3.2 Comparison with Deccan and Karoo igneous provinces

Deccan is a LIP where CFB cover an area of ~ 600,000 km^2 and mostly consist of tholeiitic basalts -locally overlain by rhyolites- that were emplaced from 63 to 68 Ma, with the main magmatic phase at 65-66 Ma (Cox and Hawkesworth, 1985; Melluso et al., 1995; 2004; 2006; Chenet et al., 2007; Sheth and Melluso, 2008; Sheth et al., 2014; Chatterjee and Bhattacharji, 2008; Keller et al., 2009; Manikyamba et al., 2015; Richards et al., 2015). The Deccan province is widely considered linked to the activation of the Reunion hot spot and was originally close to the Seychelles plateau before the opening of the Central Indian Ocean (Cox, 1989; White and McKenzie, 1989; Courtillot et al., 2003), although this view is contended by some authors (e.g., Sheth, 2005). In the paleogeographic reconstruction reported in Fig. 10 (modified after Natali et al., 2017), the Deccan traps represent part of a wider magmatic province originally extending for ~ 2000 km maximum diameter. The spatial distribution of Deccan lavas is zonally arranged with most CFB represented by LT basalts, whereas the occurrence of HT1 basaltic and picritic lavas is restricted to the NW sector. This area is located at the intersection of major NS-EW rift systems and is also characterised by the occurrence of nearly coeval alkaline-carbonatite complexes. Northeastward of the main rift systems, the CFB outcrops decrease in relation to the rapid increase of lithosphere thickness below the Bastar craton (Paul et al., 2008; Sen et al., 2009; 2012; Chalapathi Rao and Lehmann, 2011 and references therein). Reconstruction of primary CFB magmas and thermobarometric conditions using the Guddfinnsonn and Presnall (2005), Herzberg et al. (2007) and Herzberg and Asimow (2015) algorithms suggest that HT1 could be generated by T_p up to 1560°C at pressures 4-5 GPa, whereas LT were formed at lower temperature (T_p ~ 1500°C) and pressures (3-4 GPa). The thermobarometric models by Lee et al. (2009) and Putirka (2016) give temperature estimates in reasonable agreement (T_p 1500-1600°C), whereas pressures are underestimated with respect to those obtained by the Guddfinnsonn and Presnall (2005) and Herzberg et al. (2007) models (2017; Supplementary Table 1). Based on the incompatible element distribution of primary melts, Natali et al. (2017) estimated that HT1 and LT were generated by ~ 9% and 17% melting degree of a PM source, respectively.

Geochemical features of alkaline basic rocks *s.l.* coeval with CFB and related to the main rift structures (Kutch, Cambay and Narmada rifts) are reported in Fig 6 and 7, where they display a sodic affinity and variable LREE enrichment (La_N/Yb_N 13-34). As modelled for Paranà-Etendeka, Deccan alkaline primary magmas have been calculated by the Putirka (2016) model, assuming a metasomatised mantle source having mg# 0.87. Accordingly, mantle potential temperature (T_p) and pressure (P) of generation are in the range of 1370-1350°C and 2.1-2.0 GPa, respectively. Fig. 7 shows that the incompatible element patterns of Deccan alkaline magmas are analogous to those of Namibia and could be generated by similar metasomatised mantle sources, as modelled in Fig. 8.

The isotope systematics of the Deccan magmatic province is reported in Fig. 11. Similar to what was observed in the Paranà-Etendeka, HT1 picrites and the least differentiated (high-MgO) LT basalts display a restricted isotopic range (εNd from 6.8 to 2.5, $^{87}Sr/^{86}Sr_{(i)}$ 0.70386-0.70491) plotting in the upper-left quadrant of the diagram, which can be attributed to uncontaminated sublithospheric mantle components. The rest of the Deccan CFB record $^{87}Sr/^{86}Sr_{(i)}$ up to 0.71756, clearly in relation to the variable extent of crust contamination. Alkaline-carbonatite complexes show a distinctly different Sr-Nd-Pb composition with respect to CFB and a tendency towards the HIMU geochemical component, similar to those from Namibia and Angola.

The Karoo CFB province of southern Africa (and its extension in the Dronning Maud Land of Antarctica) is classically considered a LIP originated by the breakup of southern Gondwana and the opening of the south western Indian Ocean (White and McKenzie, 1989; Storey and Kyle, 1997; Elliot and Fleming, 2000; Storey et al., 2013; Riley et al., 2005; Heinonnen et al., 2014). The Karoo CFB activity mostly occurred from 174 and 184 Ma, (Hastie et al., 2014) and mainly consist of tholeiitic basalts-picrites (locally topped by rhyolites), whose variable geochemical and isotopic characteristics have been attributed either to the Sub Continental Lithospheric Mantle (SCLM, Duncan et al., 1984; Hawkesworth et al., 1984 Jourdan et al., 2007) or to mantle sources modified by plume-related asthenospheric components (Ellam and Cox, 1991; Ellam et al., 1992; Sweeney et al., 1991; 1994). As reported in Fig. 12, Karoo CFB are zonally arranged, with very high-TiO_2 (HT2) picrite-basalt lavas in the central area (Mwenetzi) and progressively lower-TiO_2 (HT1 and LT) basalts towards the periphery (Natali et al., 2017). The Guddfinnsonn and Presnall (2005), Herzberg et al. (2007) and Herzberg and Asimow (2015) algorithms applied to Karoo CFB yield T_p of 1580°C at 5GPa and 1490°C at 3-4 GPa for HT2 and LT primary magmas, respectively. Thermobarometric models by Lee et al. (2009) and Putirka (2016) give the same discrepancies observed for Paranà-Etendeka and Deccan CFB, providing comparable temperatures but systematically lower pressures (see Supplementary Table 1). Based on the incompatible element distribution of primary melts, Natali et al. (2017) estimated that LT were generated by a ~ 14%

melting degree of a PM source, whereas HT2 were generated by 8% batch melting of a PM garnet peridotite source hybridized with 15% eclogite.

Coexistent alkaline complexes occur at a triple junction located at the convergence of huge dike swarms in the Mwenetzi region. These complexes are represented by the Mashikiri nephelinites outcropping below the HT2 lavas and the ijolite-nephelinite-carbonatite complexes of Dorowa and Shawa, northward (Ellam and Cox, 1991; Harmer et al., 1998; Jourdan et al., 2007). Rocks from these complexes are the most sodic (Fig. 6) and silica undersaturated with respect to those from Paranà-Etendeka and Deccan, and according to the thermobarometric model of Putirka (2016), their primary magmas were generated at T_p of 1350-1410°C in the pressure range of 2.4-2.7 GPa (Supplementary Table 1). The PM-normalized incompatible element and the chondrite-normalized REE distribution (Fig. 7) reveal the most depressed patterns with respect to those of the other investigated provinces, the lowest LREE enrichment (La_N/Yb_N ~ 13 in Mashikiri nephelinites and ~ 5 in ijolites), as well as unusual positive anomalies in Sr and Ti. These features suggest a peculiar metasomatic enrichment of previously depleted mantle sources, quite different with respect to that envisaged for other provinces.

Sr-Nd isotopes of Karoo HT and LT, plotted in Fig. 13, display divergent trends that are partially overlapped in proximity to the Bulk Solid Earth composition, which could be attributed to the uncontaminated sublithospheric mantle of this region. The HT picrite-basalt suites display variation towards lower εNd (down to -9.7), plausibly in relation to the involvement of lithospheric components in their magma genesis. The LT suite shows a trend towards very high $^{87}Sr/^{86}Sr_{(i)}$ values, indicating a variable extent of crustal contamination. Pb isotopes also show systematic differences between LT and HT suites. Conversely, alkaline magmas are distinct in that they show an extremely unradiogenic Nd isotopic composition (εNd down to -19.9), which has been interpreted as the signature of the enriched SCLM (cf. Harmer et al., 1998).

4. Discussion and conclusions

The critical review and new elaboration of literature data on high-MgO CFB and coeval alkaline complexes from the Paranà-Etendeka LIP provide constraints on the P-T-X conditions of their mantle sources. The inception of the CFB magmatism (approximately 139 Ma) occurred in the northwestern portion of the Paranà basin and migrated southeastward towards the Etendeka region, likely in connection with a generalized northwestward lithospheric drift of this region of Gondwana over an active plume (Turner et al., 1994; Gibson et al., 2006). Whatever the extent of the lithospheric drift before the South Atlantic opening, the focus of the tectonomagmatic activity at 135-130 Ma was well-established in the Etendeka region, which comprises the oldest parts of the Walvis Ridge and several extensional lineaments that intersect the early track of the south Atlantic opening. Paleogeographic restoration shows that this region, at the centre of the CFB province, is characterised by the exclusive occurrence of high-MgO basalt-picrite rocks (belonging to both LT and HT1 suites) and is spatially/temporally (133-128 Ma) associated with alkaline-carbonatite complexes from the Ponta Grossa arch (Brazil) and Damara belt (Namibia) extensional structures.

The new petrogenetic modelling and thermobarometric estimates obtained in this work indicate that the primary magmas of the HT1 suite are the hottest and deepest CFB (T_p ~ 1590°C, P ~ 5 GPa) of the entire province. This finding conforms to the interpretation that magma generation was triggered by thermal and tectonic effects related to the impingement of a hot plume on a relatively thick continental lithosphere. The maximum temperature excess (T_{ex}), both with respect to notional MORB and local mantle xenoliths thermobarometry, is estimated as 250-300°C, in agreement with what was obtained for Deccan and Karoo (this work and Natali et al., 2017). Moreover, most high-MgO CFB of the Etendeka region show a Sr-Nd-Pb isotopic range corresponding to prevalent mantle compositions uncontaminated by lithospheric signatures, and share the “Gough” geochemical component recently recognized as the initial proto-Tristan plume activity (Hoernle et al., 2015). All of these features agree with a rapid ascent of high-MgO Etendeka magmas that, in our opinion, effectively represent the most genuine proxies of plume-related sublithospheric melts, virtually unaffected by lithospheric contamination. By contrast, out of the focal zone, most basalts of the Paranà-Etendeka CFB province are variably differentiated (MgO 9-5 wt%) and display variable increases of $^{87}Sr/^{86}Sr_{(i)}$, reflecting either lithosphere/asthenosphere mixed sources (HT1 from Paranà) and/or remarkable shallow level crustal contamination. This interpretation can reconcile the contrasting views on the role of “lithosphere” *vs* “plume” in the genesis of CFB (Turner et al., 1996; Hawkesworth et al., 2000; Gibson et al., 2000; 2006), since both views appear to be appropriate for the different CFB sections, reflecting different extents of plume-lithosphere interaction.

The Paranà-Etendeka alkaline-carbonatite complexes coeval with CFB show petrological and isotopic signatures that agree with melts from lithospheric mantle sources. The results from modelling favour the genesis of the studied alkaline magmas by moderate to low melting degrees of lithospheric mantle sources that were significantly enriched (veined?) by metasomatic phases (amphibole and phlogopite). Alkaline rocks display regional geochemical differences, suggesting distinct metasomatising events with a more relevant role of phlogopite in magma sources from south America with respect to those from southern Africa. Accordingly, the Brazilian complexes have a more potassic character and isotopic tendency to the EM1 mantle component, whereas those from Namibia and Angola display sodic affinity coupled with a signature approaching the HIMU mantle component.

On a regional scale, the main tectono magmatic characteristics of Paranà-Etendeka are also shared by Deccan and Karoo, where superheated picrite-basalt (mostly HT tholeiitic suites) and alkaline-carbonatite complexes occurred at the intersection of multiple extensional lineaments -such as faulting, rifting and dike swarms- radiating from the central area of each province (*cfr* Natali et al., 2017). As already observed for Paranà-Etendeka, the isotopic data of alkaline-carbonatite complexes of Deccan and Karoo invariably show significant differences with respect to associated high-MgO CFB, and mostly record continental lithospheric signatures. In our opinion, a satisfactory explanation for the spatial-temporal association of such contrasting, and isotopically distinct, magma types cannot be ascribed to common mantle sources, but requires the nearly contemporaneous generation of high-MgO CFB and alkaline melts from distinct mantle systems, namely the convective asthenosphere and the subcontinental lithosphere in the focal zone of LIPs. Accordingly, in the generalized tectonomagmatic model proposed in Fig. 14, the same thermal and tectonic events that characterised the axial zone of the impinging hot plume underneath the Gondwana lithosphere triggered melting of both asthenospheric and lithospheric mantle sources with magma rising through a nearly open feeding system. The results from modelling indicate that the asthenospheric peridotite solidus is crossed mostly in the range 4-5 GPa and T_p 1500-1600°C with the generation of high-MgO CFB magmas whose sources plausibly experienced adiabatic decompression and melting over a large mantle column (Gibson et al., 2000; Thompson et al., 2001; Herzberg and Asimov, 2015; Natali et al., 2016; 2017; Jennings et al., 20017). The same plume effects favoured the generation of alkaline melts by moderate to low melting degrees of the most fusible lithospheric domains (P 2-3 GPa, T 1300-1400°C), where the solidus is variably depressed due to occurrences of hydrated and/or carbonated phases; despite the small volume, alkaline melts ascended to upper crustal levels, favoured by their intrinsic low density and viscosity.

It should be noted that for LIP that do not present anomalous and focalized thermo-mechanical input on thick continental lithosphere-as in the case of the cooler CAMP and Ferrar CFB provinces-other models could be more appropriate as alternative (or complementary) to the hot plume hypothesis (Coltice et al., 2009; Hole, 2015; Natali et al., 2016).

Acknowledgments

The authors thank the Editor A. Kerr, S. Jung and an anonymous reviewer for their constructive comments that greatly improved an early version of the paper.

References

Alberti, A., Castorina, F., Censi, P., Comin-Chiaramonti, P., Gomes, C.B., 1999. Geochemical characteristics of Cretaceous carbonatites from Angola. Journal of African Earth Sciences 29, 735-759.

Azzone, R.G., Enrich, G.E.R., Gomes, C. de B., Ruberti, E., 2013. Trace element composition of parental magmas from mafic-ultramafic cumulates determined by in situ mineral analyses: The Juquiá mafic-ultramafic alkaline-carbonatite massif, SE Brazil. Journal of South American Earth Sciences 41, 5–21.

Baumgartner, M.C., Le Roex, A.P., Gurney, J.J., 2000. Mantle and crustal xenoliths from the Okenyenya lamprophyre diatreme: constraints on the upper mantle and lower crust beneath the Damara Belt, northwestern Namibia. Communications of the Geological Survey of Namibia 12, 315-327.

Beccaluva, G., Barbieri, M., Born, H., Brotzu, P., Coltorti, M., Conte, A., Garbarino, C., Gomes, C. B., Macciotta, G., Morbidelli L., Ruberti, E., Siena, F., Traversa, G., 1992. Fractional Crystallization and liquid immiscibilità processes in the Alkaline-Carbonatite complex of Juquià (São Paulo, Brazil). Journal of Petrology 33, 1371–1404.

Beccaluva, L., Azzouni-Sekkal, A., Benhallou, A., Bianchini, G., Ellam, R.M., Marzola, M., Siena, F., Stuart F.M., 2007. Intracratonic asthenosphere upwelling and lithosphere rejuvenation beneath the Hoggar swell (Algeria): evidence from HIMU metasomatised lherzolite mantle xenoliths. Earth and Planetary Science Letters 260, 482–494.

Beccaluva, L., Bianchini, G., Ellam, R.M., Marzola, M., Oun, K.M., Siena, F., Stuart, F.M., 2008. The role of HIMU metasomatic components in the African lithospheric mantle: petrological evidence from the Gharyan peridotite xenoliths, NW Libya. Geological Society of London, Special Publications 293, 253–277.

Beccaluva, L., Bianchini, G., Natali, C., Siena F., 2009. Continental Flood Basalts and Mantle Plumes: a Case Study of the Northern Ethiopian Plateau. Journal of Petrology 50, 1377-1403.

Beccaluva, L., Bianchini, G., Ellam, R.M., Natali, C., Santato, A., Siena, F., Stuart, F.M., 2011. Peridotite xenoliths from Ethiopia: inferences about mantle processes from plume to rift settings. Geological Society of America (GSA) Special Paper 478, pp. 77–104.

Beccaluva, L., Bianchini, G., Natali, C., Siena, F., 2017. The alkaline-carbonatite complex of Jacupiranga (Brazil): magma genesis and mode of emplacement. Gondwana Research 44, 157-177.

Bell, K., 2001. Carbonatites: Relationships with mantle-plume activity. Geological Society of America (GSA) Special Paper 352, pp. 267–290.

Bellieni, G., Comin-Chiaramonti, P., Marques, L.S., Melfi, A.J., Nardy, A.J.R., Papatrechas, C., Piccirillo, E.M., Roisenberg, A., 1986. Petrogenetic aspects of acid and basaltic lavas from the Paranà plateau (Brazil): geological, mineralogical and petrochemical relationships. Journal of Petrology 27, 915-944.

Bianchini, G., Bryce, J.G., Blichert-Toft, J., Beccaluva, L., Natali, C., 2014. Mantle dynamics and secular variations beneath the East African Rift: Insights from peridotite xenoliths (Mega, Ethiopia). Chemical Geology 386, 49-58.

Bizzi, L.A., De Wit, M.J., Smith, C.B., McDonald, I., Armstrong, R.A., 1995. Heterogeneous enriched mantle materials and Dupal-type magmatism along the SW margin of the São Francisco craton, Brazil. Journal of Geodynamics 20, 469-491.

Campbell, I.H., 2001. Identification of ancient mantle plumes. GSA Special Paper 352, pp. 5 – 21.

Campbell, I.H., Davies G.F., 2006. Do mantle plumes exist? Episodes 29, 162–168.

Campbell, I.H., 2007. Testing the plume theory. Chemical Geology 241, 153–176.

Cernuschi, F., Dilles, J.H., Kent, A.J.R., Schroer, G., Raab, A.K., Conti, B., Muzio, R., 2015. Geology, geochemistry and geochronology of the Cretaceous Lascano East intrusive complex and magmatic evolution of the Laguna Merìnbasin, Uruguay. Gondwana Research 28, 837-857.

Chalapathi Rao, N.V., Lehmann, B., 2011. Kimberlites, flood basalts and mantle plumes: new insights from the Deccan Large Igneous Province. Earth-Science Reviews 107, 315–324.

Chatterjee, N., Bhattacharji, S., 2008. Trace element variations in Deccan basalts: roles of mantle melting, fractional crystallization and crustal assimilation. Journal of the Geological Society of India 71, 171–188.

Chenet, A-L., Quidelleur, X., Fluteau, F., Courtillot, V., Bajpai, S., 2007. ^{40}K-^{40}Ar dating of the Main Deccan large igneous province: Further evidence of KTB age and short duration. Earth and Planetary Science Letters 263, 1–15.

Coltice, N., Bertrand, H., Rey, P., Jourdan, F., Phillips, B.R., Ricard Y., 2009. Global warming of the mantle beneath continents back to the Archaean. Gondwana Research 15, 254–266.

Coltorti, M., Alberti, A., Beccaluva, L., Dos Santos, A.B., Mazzucchelli, M., Morais, E., Rivalenti, G., Siena, F., 1993. The Tchivira-Bonga alkaline-carbonatite complex (Angola): petrological study and comparison with some Brazilian analogues. European Journal of Mineralogy 5, 1001–1024.

Comin-Chiaramonti, P., Gomes, C. B., (eds.) 2005. Mesozoic to Cenozoic alkaline magmatism in the Brazilian Platform. Editora da Universidade de São Paulo, 755 pp.

Comin-Chiaramonti, P., Gomes, C.B., Castorina, F., Censi P., Antonini, P., Furtado, S., Ruberti , E., Scheibe, L.F., 2002. Anitápolis and Lages alkaline-carbonatite complexes, Santa Catarina State, Brazil: geochemistry and geodynamic implications. Revista Brasileira de Geociências 32, 639-653.

Comin-Chiaramonti, P., Marzoli, A., Gomes, C. B., Milan, A., Riccomini, C., Mantovani, M.M.S., Renne, P., Tassinari, C.C.G., Vasconcelos, P.M., 2007. Origin of Post Paleozoic Magmatism in Eastern Paraguay. Geological Society of America (GSA) Special Paper 430, pp. 603-633.

Comin-Chiaramonti, P., De Min, A., Girardi, V.A.V., Ruberti, E., 2011. Post-Paleozoic magmatism in Angola and Namibia: A review. Geological Society of America (GSA) Special Paper 478, pp. 223-247.

Comin-Chiaramonti, P., De Min, A., Girardi, V.A.V., Gomes, C. B., 2014. Carbonatites and primary carbonates in the Rio Apa and Amambay regions, NE Paraguay. Lithos 188, 84–96.

Cordani, U.G., Sartori, P.L., Kawashita, K., 1980. Geoquímica dos isótopos de estrôncio e a evolução da atividade vulcânica na Bacia do Paraná (Sul do Brasil) durante o Cretáceo. Anais da Academia Brasileira de Ciências 52, 811–818.

Courtillot, V., Davaille, A., Besse J., Stock, J., 2003. Three distinct types of hotspots in the Earth's mantle. Earth and Planetary Science Letters 205, 295-308.

Cox, K.G., 1989. The role of mantle plumes in the development of continental drainage patterns. Nature 342, 873-877.

Cox, K.G., Hawkesworth, C.J., 1985. Geochemical Stratigraphy of the Deccan Traps at Mahabaleshwar, Western Ghats, India, with Implications for Open System Magmatic Processes. Journal of Petrology 26, 355-377.

Dasgupta, R., Hirschmann, M.M., Smith, N.D., 2007. Partial Melting Experiments of Peridotite + CO_2 at 3 GPa and Genesis of Alkalic Ocean Island Basalts. Journal of Petrology 48, 2093–2124.

Danyushevsky, L.V., Plechov, V., 2011. Petrolog3: Integrated software for modeling crystallization processes. Geochemistry, Geophysics, Geosystems 12, doi:10.1029/2011GC003516.

de Bruiyn, H., Schoch, A.E., Fairwood, D.S., van der Westhuizen W.A., 2005. The geology and petrochemistry of the Mashikiri Formation along the Olifants River Section, Kruger National Park, South Africa. South African Journal of Geology 108, 173-186.

Dessai, A.G., Markwick, A., Vaselli, O., Downes, H., 2004. Granulite and pyroxenite xenoliths from the Deccan Trap. insight into the nature and composition of the lower lithosphere beneath cratonic India: Lithos 78, 263-290.

Duncan, A.R., Erlank, A.J., Marsh, J.S., 1984. Regional geochemistry of the Karoo igneous province. In: A.J. Erlank (Eds), Petrogenesis of the volcanic rocks of the Karoo province. Special Publication of the Geological Society of South Africa 13, pp. 355-388.

Ellam, R.M., Cox, K.G., 1991. An interpretation of Karoo picrite basalts in terms of interaction between asthenospheric magmas and the mantle lithosphere: Earth and Planetary Science Letters 105, 330-342.

Ellam, R.M., Carlson, R.W., Shirey, S.B., 1992. Evidence from Re-Os isotopes for plume lithosphere mixing in Karoo flood basalt genesis. Nature, 359, 718-721.

Elliot, D.H., Fleming, T.H., 2000. Weddell triple junction: the principal focus of Ferrar and Karoo magmatism during initial break-up of Gondwana. Geology, 28, 539 – 542.

Ernesto, M., Marques, L.S., Piccirillo, E.M., Molina, E.C., Ussami, N., Comin-Chiaramonti, P., Bellieni, G., 2002. Paraná Magmatic Province-Tristan da Cunha plume system: fixed versus mobile plume, petrogenetic considerations and alternative heat sources. Journal of Volcanology and Geothermal Research 118, 15-36.

Ernst, R.E., Bell, K., 2010. Large Igneous Provinces (LIPs) and carbonatites. Mineralogy and Petrology 98, 55-76.

Fodor, R.V., Sial, A.N., Gandhok, G., 2002. Petrology of spinel peridotite xenoliths from northeastern Brazil: lithosphere with a high geothermal gradient imparted by Fernando de Noronha plume. Journal of South American Earth Sciences 15, 199-214.

Gibson, S.A., Thompson, R.N., Dickin, A.P., Leonardos, O.H., 1995. High-Ti and low-Ti mafic potassic magmas: key to plume-lithosphere interactions and continental flood-basalt genesis. Earth and Planetary Science Letters 136, 149-165.

Gibson, S.A., Thompson, R.N., Dickin, A.P., 2000. Ferropicrites: geochemical evidence for Fe-rich streaks in upwelling mantle plumes. Earth and Planetary Science Letters 174, 355–374.

Gibson, S.A., Thompson, R.N., Day, J.A., 2006. Timescales and mechanisms of plume-lithosphere interactions: $^{40}Ar/^{39}Ar$ geochronology and geochemistry of alkaline igneous rocks from the Paraná-Etendeka large igneous province: Earth and Planetary Science Letters 251, 1–17.

Gomes, C.B., Ruberti, E., Comin-Chiaramonti, P., Azzone, R.G., 2011. Alkaline magmatism in the Ponta Grossa Arch, SE Brazil: A review. Journal of South American Earth Sciences, 32, 152–168.

Green, D.H., Fallon, T.J., 2005. Primary magmas at mid-ocean ridges, “hotspots”, and other intraplate settings: constraints on mantle potential temperature. Geological Society of America (GSA) Special Paper 388, pp. 217–247.

Griffin, W.L., O'Reilly, S.Y., Natapov, L.M., Ryan, C.G., 2003. The evolution of lithospheric mantle beneath the Kalahari Craton and its margins. Lithos 71, 215-241.

Guarino, V., Wu, F.-Y., Lustrino, M., Melluso, L., Bratzu, P., Gomes, C.d.B., Ruberti, E., Tassinari, C.C.G., Svisero, D.P., 2013. U-Pb ages, Sr-Nd isotope geochemistry, and petrogenesis of kimberlites, kamafugites and pholgopite-picrites of the Alto Paranaiba Igneous Province, Brazil. Chemical Geology 353, 65–82.

Gudfinnsson, G.H., Presnall, D.C., 2005. Continuous gradations among primary carbonatitic, kimberlitic, melilitic, basaltic, picritic and komatiitic melts in equilibrium with garnet lherzolite at 3–8 GPa. Journal of Petrology 46, 1646–1659.

Harmer, R.E., Lee, C.A., Eglington, B.M., 1998. A deep mantle source for carbonatite magmatism: evidence from the nephelinites and carbonatites of the Buhera district, SE Zimbabwe. Earth and Planetary Science Letters 158, 131-142.

Harris, C., Marsh, J.S., Milner, S.C. 1999. Petrology of the alkaline core of the Messum igneous complex, Namibia: evidence for the progressively decreasing effect of crustal contamination. Journal of Petrology 40, 1377-1397.

Hastie, W.W., Watkeys, M.K., Aubourg, C., 2014. Magma flow in dyke swarms of the Karoo LIP: Implications for the mantle plume hypothesis. Gondwana Research, 25, 736-755.

Hawkesworth, C.J., Marsh, J.S., Duncan, A.R., Erlank, A.J., Norry, M.J., 1984. The role of continental lithosphere in the generation of the Karoo volcanic rocks: evidence from combined Nd- and Sr-isotope studies. Special Publication of the Geological Society of South Africa 13, pp. 341-354.

Hawkesworth, C. J., Gallagher, K., Kelley, S., Mantovani, M, Peate, D.W., Regelous, M., Rogers, N.W., 1992. Paraná magmatism and the opening of the South Atlantic. London Geological Society (GSL) Special Publications 68, pp. 221-240.

Hawkesworth, C.J., Gallagher, K., Kirstein, L., Mantovani, M.S.M., Peate, D.W., Turner, S., 2000. Tectonic controls on magmatism associated with continental break-up: an example from the Paraná–Etendeka Province. Earth and Planetary Science Letters 179, 335–349.

Heinonen, J.S., Carlson, R.W., Riley, T.R., Luttinen, A.V., Horan, M.F., 2014. Subduction-modified oceanic crust mixed with a depleted mantle reservoir in the sources of the Karoo continental flood basalt province. Earth and Planetary Science Letters 394, 229-241.

Herzberg, C., Asimow, P.D., Arndt, N., Niu, Y., Lesher, C.M., Fitton, J.G., Cheadle, M.J., Saunders, A.D., 2007. Temperatures in ambient mantle and plumes: Constraints from basalts, picrites and komatiites: Geochemistry Geophysics Geosystems 8, doi:10.1029GC001390.

Herzberg, C., Asimow, P.D., 2015. PRIMELT3MEGA.XLSM software for primary magma calculation: Peridotite primary magma MgO contents from the liquidus to the solidus. Geochemistry, Geophysics, Geosystems 8, doi:10.1002/2014GC005631.

Hoernle, K., Rohde, J., Hauff, F., Garbe-Schönberg, D., Homrighausen, S., Werner, R., Morgan, J.P., 2015. How and when plume zonation appeared during the 132 Myr evolution of the Tristan hotspot. Nature Communications 6, 7799, doi:10.1038/ncomms8799.

Hofmann, A.W., 1997. Mantle geochemistry: the message from oceanic volcanism. Nature 385, 219-229.

Hole, M.J., 2015. The generation of continental flood basalts by decompression melting of internally heated mantle. Geology 43, 311–314.

Huang, J.M., Hawkesworth, C.J., van Calsteren, P.W.C., McDermott, F., 1995. Geochemical characteristics and origin of the Jacupiranga carbonatites, Brazil. Chemical Geology 119, 79–99.

Iacumin, M., De Min, A., Piccirillo, E.M., Bellieni, G., 2003. Source mantle heterogeneity and its role in the genesis of Late Archean-Proterozoic (2.7-1.0 Ga) and Mesozoic (200 and 130 Ma) tholeiitic magmatism in the south American Platform. Earth-Science Reviews 62, 365-397.

Janasi, VA, Freitas, VA, Heaman, LH., 2011. The onset of flood volcanism, Northern Paraná Basin, Brazil: A precise U-Pb baddeleyite/zircon age for a Chapecó-type dacite. Earth Planetary Science Letters 302, 147-153.

Jennings, E.S., Gibson, S.A., Maclennan, J., Heinonen, J.S., 2017. Deep mixing of mantle melts beneath continental flood basalt provinces: Constraints from olivine-hosted melt inclusions in primitive magmas. Geochimica et Cosmochimica Acta 196, 36-57.

Jourdan, F., Bertrand, H., Sharer, U., Blichert-Toft, Féraud, G., Kampunzu, A.B., Le Gall, B., Watkeys, M.K., 2007. Major-trace element and Sr-Nd-Hf-Pb isotope compositions of the Karoo large igneous province in Botswana-Zimbabwe. Journal of Petrology 48, 1043-1077.

Jung, S., Pfänder, J.A., Brauns, M., Maas, R., 2011. Crustal contamination and mantle source characteristics in continental intra-plate volcanic rocks: Pb, Hf and Os isotopes from central European volcanic province basalts. Geochimica et Cosmochimica Acta, 75 2664–2683.

Karmalkar, N.R., Duraiswami, R.A., Chalapathi Rao, N.V., Paul, D.K., 2009. Mantle-derived mafic-ultramafic xenoliths and the nature of Indian sub-continental lithosphere. Journal of the Geological Society of India 73, 657–679.

Keller, G., Adatte, T., Bajpai, S., Mohabey, D.M., Widdowson, M., Khosla, A., Sharma, R., Khosla, S.C., Gertsch, B., Fleitman, D., Sahni, A., 2009. K-T transition in Deccan Traps of Central India marks major marine seaway across India. Earth and Planetary Science Letters 282, 10–23.

Lee, C.-T.,A., Luffi, P., Plank, T., Dalton, H., Leeman, W.P., 2009. Constraints on the depths and temperatures of basaltic magma generation on Earth and other terrestrial planets using new thermobarometers for mafic magmas. Earth and Planetary Science Letters 279, 20–33.

Le Roex, A.P., Lanyon, R., 1998. Isotope and trace element geochemistry of Cretaceous Damaraland lamprophyres and carbonatites, Northwest Namibia: evidence for plume–lithosphere interactions. Journal of Petrology 39, 1117–1146.

Le Roex, A.P., Class, C., 2014. Metasomatism of the Pan-African lithospheric mantle beneath the Damara Belt, Namibia, by the Tristan mantle plume: geochemical evidence from mantle xenoliths. Contribution to Mineralogy and Petrology 168: 1046.

Lustrino, M., Melluso, L., Brotzu, P., Gomes, C. B., Morbidelli, L., Muzio, R., Ruberti, E., Tassinari, C.C.G., 2005. Petrogenesis of the early Cretaceous Valle Chico igneous complex (SE Uruguay): relationship with Paraná–Etendeka magmatism. Lithos 82, 407–434.

Manikyamba, C., Ganguly, S., Santosh, M., Singh, M.R., Saha, A., 2015. Arc-nascent back-arc signature in meta basalts from the Neoarchean Jonnagiri greenstone terrane, eastern Dharwar Craton, India. Geological Journal 50, 651-669.

Marsh, J.S., Swart, R., 2016. The Bero Volcanic Complex: Extension of the Paraná-Etendeka Igneous Province into SW Angola. Journal of Volcanology and Geothermal Research (in press).

Marzoli, A., Renne, P.R., Piccirillo, E.M., Ernesto, M., Bellieni, G., De Min, A., 1999. Extensive 200-million-year-old continental flood basalts of the Central Atlantic magmatic province. Science 284, 616–618.

Melluso, L., Beccaluva, L., Brotzu, P., Gregnanin, A., Gupta, A.K., Morbidelli, L., Traversa, G., 1995. Constraints on the mantle sources of the Deccan Traps from the petrology and geochemistry of the basalts of Gujarat State (Western India). Journal of Petrology 36, 1393–1432.

Melluso, L., Barbieri, M., Beccaluva, L., 2004. Chemical evolution, petrogenesis, and regional chemical correlations of the flood basalt sequence in the central Deccan Traps, India. Proceedings of the Indian Academy of Science 113, 1-18.

Melluso, L., Mahoney, J.J., Dallai, L., 2006. Mantle sources and crustal input in Mg-rich Deccan Trap basalts from Gujarat (India). Lithos 89, 259–274.

Middlemost, E.A.K., 1975. The basalt clan. Earth-Science Review 11, 337-364.

Milner, S.C., Le Roex, A.P., 1996. Isotope characteristics of the Okenyenya igneous complex, northwestern Namibia: Constraints on the composition of the early Tristan plume and the origin of the EM 1 mantle component. Earth and Planetary Science Letters 141, 277-291.

Morbidelli, L., Gomes, C.B., Beccaluva, L., Brotzu, P., Conte, A., Ruberti, E., Traversa, G., 1995. Mineralogical, petrological and geochemical aspects of alkaline and alkaline-carbonatite associations from Brazil. Earth-Science Reviews 39, 135–168.

Morris, E.M., Pasteris, J.D., 1987. Mantle Metasomatism and Alkaline Magmatism. Boulder: Geological Society of America, Special Paper 215, pp 383.

Natali, C., Beccaluva, G., Bianchini, G., Ellam, R.M., Siena, F., Stuart, F., 2013. Carbonated alkali-silicate metasomatism in the North Africa lithosphere: Evidence from Middle Atlas spinel-lherzolites, Morocco. Journal of South American Earth Sciences 41, 113–121.

Natali, C., Beccaluva, G., Bianchini, G., Ellam, R.M., Savo, A., Siena, F., Stuart, F.M., 2016. High-MgO lavas associated to CFB as indicators of plume-related thermochemical effects: The case of ultra-titaniferous picrite–basalt from the Northern Ethiopian–Yemeni Plateau. Gondwana Research 34, 29-48.

Natali, C., Beccaluva, G., Bianchini, G., Siena, F., 2017. Comparison among Ethiopia-Yemen, Deccan, and Karoo continental flood basalts of central Gondwana: Insights on lithosphere versus asthenosphere contributions in compositionally zoned magmatic provinces. Geological Society of America (GSA) Special Paper 526, 191-215.

Nielson, J.E., Wilshire, H.G., 1993. Magma transport and metasomatism in the mantle: a critical review of current geochemical models. American Mineralogist 78, 1117-1134.

Owen-Smith, T.M., Ashwal, L.D., Sudo, M., Trumbull, R., 2017. Age and petrogenesis of the Doros Complex, Namibia, and implications for early plume-derived melts in the Paraná–Etendeka LIP. Journal of Petrology 58, 423-442.

Paul, D.K., Ray, A., Das, B., Patil, S.K., Biswas, S.K., 2008. Petrology, geochemistry and paleomagnetism of the earliest magmatic rocks of Deccan Volcanic Province, Kutch, Northwest India. Lithos 102, 237-259.

Peate, D.W., Hawkesworth, C.J., Mantovani, M.S.M., Rogers, N.W., Turner, S.P., 1999. Petrogenesis and stratigraphy of the high-Ti/Y Urubici magma type in the Paraná flood basalt province and implications for the nature of ‘Dupal’- type mantle in the South Atlantic region. Journal of Petrology 40, 451-473.

Piccirillo, E.M., Melfi, A.J., 1988. The Mesozoic flood volcanism of the Paranà basin: petrogenetic and geophysical aspects IAG-USP press, São Paulo, pp. 600.

Piccirillo, E.M., Civetta, L., Petrini, R., Longinelli, A., Bellieni, G., Comin-Chiaramonti, P., Marques, L.S., Melfi, A.J., 1989. Regional variations within the Paraná flood basalts (southern Brazil): evidence for subcontinental mantle heterogeneity and crustal contamination. Chemical Geology 75, 103–122.

Piccirillo, E.M., Bellieni, G., Cavazzini, G., Comin-Chiaramonti, P., Petrini, R., Melfi, A.J., Pinese, J.P.P., Zantadeschi, P., De Min, A., 1990. Lower Cretaceous tholeiitic dyke swarms from the Ponta Grossa arch (southeast Brazil): Petrology, Sr-Nd isotopes and genetic relationships with the Paraná flood volcanics. Chemical Geology 89, 19-48.

Pilet S., Baker, M.B., Stolper, E.M., 2008. Metasomatized lithosphere and the origin of alkaline lavas. Science 320, 916-919.

Pilet, S., Baker, M.B., Muntener, O., Stolper, E.M., 2011. Monte Carlo simulations of metasomatic enrichment in the lithosphere and implications for the source of alkaline basalts. Journal of Petrology 52, 1415–1442.

Pinto, V.M., Hartmann, L.A., Santos, J.O.S., McNaughton, N.J., Wildner, W., 2011. Zircon U-Pb geochronology from the Paranà bimodal volcanic province support a brief eruptive cycle at ~135 Ma. Chemical Geology 281, 93-102.

Pirajno, F., 2015. Intracontinental anorogenic alkaline magmatism and carbonatites associated mineral systems and the mantle plume connection. Gondwana Research 27, 1181-1216.

Putirka, K., 2016. Rates and styles of planetary cooling on Earth, Moon, Mars and Vesta, using new models for oxygen fugacity, ferric-ferrous ratios, olivine-liquid Fe-Mg exchange, and mantle potential temperature. American Mineralogist 101, 819-840

Rämö, O.T., Heikkilä, P.A., Pulkkinen, A.H., 2016. Geochemistry of Paraná-Etendeka basalts from Misiones, Argentina: Some new insights into the petrogenesis of high-Ti continental flood basalts. Journal of South American Earth Sciences 67, 25-39.

Renne, P.R., Deckart, K., Ernesto, M., Féraud, G., Piccirillo, E.M., 1996a. Age of the Ponta Grossa dike swarm (Brazil), and implications to Paraná flood volcanism: Earth and Planetary Science Letters 144, 199–211.

Renne, P.R., Glen, J.M., Milner, S.C., Duncan, A.R., 1996b. Age of Etendeka flood volcanism and associated intrusions in southwestern Africa. Geology 24, 659–662.

Richards, M.A., Alvarez, W., Self, S., Karlstrom, L., Renne, P.R., Manga, M., Sprain, C.J., Smit, J., Vanderkluysen, L., Gibson, S.A., 2015, Triggering of the largest Deccan eruptions by the Chicxulub impact: Geological Society of America Bulletin 127, 11–12.

Riley, T.R., Leat, P.T., Curtis, M.L., Millar, L.L., Fazel, A., 2005. Early–Middle Jurassic dolerite dykes from western Dronning Maud Land (Antarctica): identifying mantle sources in the Karoo large igneous province: Journal of Petrology 46, 1489–1524.

Rivalenti, G., Mazzucchelli, M., Girardi, V.A.V., Vannucci, R., Barbieri, M.A., Zanetti, A., Goldstein, S.L., 2000. Composition and processes of the mantle lithosphere in northeastern Brazil and Fernando de Noronha: evidence from mantle xenoliths. Contribution to Mineralogy and Petrology 138, 308-325.

Rocha-Junior, E.R.V., Marques, L. S., Babinski, M., Nardy, A.J.R., Figueiredo A.M.G., Machado, F.B., 2013. Sr-Nd-Pb isotopic constraints on the nature of the mantle sources involved in the genesis of the high-Ti tholeiites from northern Paranà Continental Flood Basalts (Brazil). Journal of South American Earth Sciences 46, 9–25.

Rooney, T.O., Nelson, W.R., Ayalew, D., Hanan, B., Yirgu, G., Kappelman, J., 2017. Melting the lithosphere: Metasomes as a source for mantle-derived magmas. Earth and Planetary Science Letters 461, 105–118.

Ruberti, E., Gomes, C.B. Comin-Chiaramonti, P., 2005. The alkaline magmatism from Ponta Grossa Arch. In: Comin-Chiaramonti P. and Gomes C.B. (Eds.), Mesozoic to Cenozoic alkaline magmatism in the Brazilian platform. Edusp/Fapesp, São Paulo, Brazil, 473-522.

Safonova, I.Yu., Santosh, M. 2014. Accretion complexes in the Asia-Pacific region: Tracing archives of ocean plate stratigraphy and tracking mantle plumes. Gondwana Research 25, 126-158.

Sgualdo, P., Aviado, K., Beccaluva, L., Bianchini, G., Blichert-Toft, J., Bryce, J.G., Graham, D.W., Natali, C., Siena, F., 2015. Lithospheric mantle evolution in the Afro-Arabian domain: Insights from Bir Ali mantle xenoliths (Yemen). Tectonophysics 650, 3-17.

Sen, A., Pande, K., Hegner, E., Sharma, K.K., Dayal, A.M., Sheth, H.C., Mistry, H., 2012. Deccan volcanism in Rajasthan: ^{40}Ar-^{39}Ar geochronology and geochemistry of the Tavidar volcanic suite. Journal of Asian Earth Sciences 59, 127-140.

Sen, G., Bizimis, M., Das, R., Paul D.K., Ray, A., Biswas, S., 2009. Deccan plume, lithosphere rifting, and volcanism in Kutch, India. Earth and Planetary Science Letters 277, 101–111.

Shervais, J.W., Taylor, L.A., Lugmair, G.W., Clayton, R.N., Mayeda, T.K., Korotev, R.L., 1988. Early Proterozoic oceanic crust and the evolution of subcontinental mantle: Eclogites and related rocks from southern Africa, Geological Society of America Bullettin 100, 411-423.

Sheth, H., 2005. From Deccan to Reunion: no trace of a mantle plume. Geological Society of America (GSA) Special Papers 388, pp. 477–501.

Sheth, H., Melluso, L., 2008. The Mount Pavagadh volcanic suite, Deccan traps: geochemical stratigraphy and magmatic evolution. Journal of Asian Earth Sciences 32, 5–21.

Sheth, H.C. Zellmer, G.F., Demonterova, E.I., Ivanov, A.V., Kumar, R., Kumar Patel, R., 2014. The Deccan tholeiite lavas and dykes of Ghatkopar-Powai area, Mumbai, Panvel flexure zone: Geochemistry, stratigraphic status, and tectonic significance. Journal of Asian Earth Sciences 84, 69-82.

Simonetti, A., Bell, K., Viladkar, S.G., 1995. Isotopic data from the Amba Dongar Carbonatite Complex, west-central India: Evidence for an enriched mantle source. Chemical Geology (Isotope Geoscience Section) 122, 185-198.

Simonetti, A., Goldstein, S.L., Schmidberger, S.S., Viladkar , S.G., 1998. Geochemical and Nd, Pb, and Sr Isotope Data from Deccan Alkaline Complexes— Inferences for Mantle Sources and Plume-Lithosphere Interaction, Journal of Petrology 39, 1847-1864.

Späth, A., Le Roex, A.P., Opiyo-Akech, N., 2001. Plume–Lithosphere Interaction and the Origin of Continental Rift-related Alkaline Volcanism—the Chyulu Hills Volcanic Province, Southern Kenya. Journal of Petrology 42, 765-787.

Stanley, J.R., Flowers, R.M., Bell, D.R., 2015. Erosion patterns and mantle sources of topographic change across the southern African Plateau derived from the shallow and deep records of kimberlites. Geochemistry, Geophysics, Geosystems 16, 3235-3256.

Storey, B.C., Vaughan, A.P.M., Riley, T.R., 2013. The links between large igneous provinces, continental break-up and environmental change: evidence reviewed from Antarctica. Earth and Environmental Science Transactions of the Royal Society of Edinburgh 104, 17-30.

Storey, B.C., and Kyle, P.R., 1997. An active mantle mechanism for Gondwana break-up. South African Journal of Geology 100, 283–290.

Stracke, A., 2012. Earth's heterogeneous mantle: A product of convection-driven interaction between crust and mantle. Chemical Geology 330-331, 274-299.

Stewart, K., Turner, S., Kelley, S., Hawkesworth, C., Kirstein, L., Mantovani, M., 1996. 3-D, ^{40}Ar-^{39}Ar geochronology in the Paraná continental flood basalt province: Earth and Planetary Science Letters 143, 95–109.

Sun, S.S., McDonough, W.F., 1989. Chemical and isotopic systematics of oceanic basalts: implications for mantle composition and processes. Geological Society of London (GSL) Special Publications 42, pp. 313-347.

Sweeney, R.J., Fallon, T.J., Green, D.H., Tatsumi, Y., 1991. The mantle origins of Karoo picrites. Earth and Planetary Science Letters 107, 256-271.

Sweeney, R.J., Duncan, A.R., Erlank, A.J., 1994. Geochemistry and petrogenesis of Central Lebombo basalts from the Karoo Igneous Province. Journal of Petrology, 35, 95-125.

Thiede, D.S., Vasconcelos, P.M., 2010. Paraná flood basalts: rapid extrusion hypothesis confirmed by new $^{40}Ar/^{39}Ar$ results. Geology 38, 747–750.

Thompson, R.N., Gibson, S.A., 2000. Transient high temperatures in mantle plume heads inferred from magnesian olivines in Phanerozoic picrites. Nature 407, 502–506.

Thompson, R.N., Gibson, S.A., Dickin, A.P., Smith, P.M., 2001. Early Cretaceous basalt and picrite dikes of the southern Etendeka region, NW Namibia: Windows into the role of the Tristan mantle plume in Paraná–Etendeka magmatism: Journal of Petrology 42, 2049–2081.

Trumbull, R.B., Bühn, B., Romer, R.L., Volker, F., 2003. The petrology of basanite-tephrite intrusions in the Erongo complex and implications for a plume source of Cretaceous alkaline complexes in Namibia. Journal of Petrology 44, 93–112.

Trumbull, R.B., Reid, D.L., de Beer, C., van Acken, D., Romer, R.L., 2007. Magmatism and continental breakup at the west margin of southern Africa: a geochemical comparison of dolerite dikes from northwestern Namibia and the Western Cape. South African Journal of Geology 110, 477-502.

Tuff, J., Takahashi, E., Gibson, S.A., 2005. Experimental constraints on the role of garnet pyroxenite in the in the genesis of High-Fe mantle plume derived melts. Journal of Petrology 46, 2223-2258.

Turner, S., Regelous, M., Kelly, S., Hawkesworth, C., Mantovani, M., 1994. Magmatism and continental break-up in the South Atlantic: $^{40}Ar/^{39}Ar$ geochronology. Earth and Planetary Science Letters 121, 333-348.

Turner, S.P., Hawkesworth, C.J., Gallagher, K., Stewart, K., Peate, D.W., Mantovani, M.S.M., 1996. Mantle plumes, flood basalts and thermal models for melt generation beneath continents: assessment of a conductive heating model and application to the Paraná. Journal of Geophysical Research 101, 11503–11518.

Walter, M.J., 1998. Melting of garnet peridotite and the origin of komatiite and depleted lithosphere. Journal of Petrology 39, 29-60.

White, R.W., McKenzie, D.P., 1989. Magmatism at rift zones: the generation of volcanic continental margins and flood basalts. Journal of Geophysical Research 94, 7685-7729.

White, R.W., McKenzie, D.P., 1995. Mantle plumes and flood basalts. Journal of Geophysical Reasearch 100, 17543–17585.

Zindler, A., Hart, S., 1986. Chemical geodynamics. Annual Review of Earth and Planetary Sciences 14, 493–571.

Figure captions

Figure 1 – Paleogeographic reconstruction of Parana-Etendeka CFB at 135-130 Ma (modified after White and McKenzie, 1989). Low-Ti (LT) and high-Ti (HT1) spatial distribution was reviewed after data from Piccirillo and Melfi (1988), Piccirillo et al. (1990), Hawkesworth et al. (1992), Peate et al. (1999), Marzoli et al. (1999), Thompson et al. (2001), Lustrino et al. (2005), Cernuschi et al. (2015), Marsh and Swart (2016), Rämö et al. (2016). Locations of Early Cretaceous alkaline-carbonatite complexes after Beccaluva et al. (1992; 2017), Coltorti et al. (1993), Trumbull et al. (2003), Comin-Chiaramonti and Gomes (2005), Gibson et al. (2006), Comin-Chiaramonti et al.

(2011; 2014) and references therein, Gomes et al. (2011) and references therein. The hot spot focal zone includes the oldest part of the Walvis volcanic ridge and the Etendeka high-MgO rocks (max T_p 1590°C) and is considered the axis of the Proto-Tristan mantle plume during the main magmatic phase of the Paranà-Etendeka province; it also includes the majority of coeval alkaline-carbonatite complexes, along the extensional structures that intersect the early track of the south Atlantic opening.

Figure 2 – FeO_t, TiO_2, Nb and Ce *vs* MgO variation diagrams for the Paranà-Etendeka CFB. Data from the GEOROC database (http://georoc.mpch-mainz.gwdg.de/georoc/) and by Owen-Smith et al. (2017). LT type localities are Esmeralda, Gramado in Paranà and Horingbaai, Tafelberg in Etendeka. HT1 type localities are Paranapanema, Pitanga, Urubici in Paranà and Khumib, Doros in Etendeka. Empirical boundaries between LT and HT1 CFB are drawn in order to minimise the misclassified samples (generally less than 5%).

Figure 3 – Chondrite-normalized Rare Earth Element (REE) patterns for LT and HT1 Paranà-Etendeka CFB. Average La_N/Yb_N for each group are also reported. Normalizing factors are from Sun and McDonough (1989). Data are from the GEOROC database and from Owen-Smith et al. (2017).

Figure 4 – MgO *vs* FeO diagram for the Paranà-Etendeka CFB. HT1 and LT primary magmas were modelled according to Herzberg and Asimow (2015). Liquid lines of descent were modelled according to Petrolog software v.3 (Danyuschevsky and Pletchov, 2011). Data are from the GEOROC database and from Owen-Smith et al. (2017). Abbreviations: Ol = olivine, Cpx = clinopyroxene; Pl = plagioclase.

Figure 5 – Incompatible element distribution of calculated LT and HT1 primary melts (data from Ewart et al., 1998; Gibson et al., 2000) and modelled composition obtained by batch melting of a PM source hybridized with 3% eclogite. Source mode and melting proportions conform to experimental data by Walter (1998); partition coefficients (*Kd*) from the GERM database. Normalizing factors are from Sun and McDonough (1989). See text for further explanation.

Figure 6 – Na_2O *vs* K_2O (wt%) binary diagram for mafic rocks from alkaline-carbonatite complexes coeval with CFB from the a) Paranà-Etendeka, b) Deccan and c) Karoo igneous provinces. Subdivision among various sodic and potassic affinities are from Middlemost (1975). Paranà-Etendeka data are from Beccaluva et al. (1992; 2017), Coltorti et al. (1993), Trumbull et al. (2003), Comin-Chiaramonti et al. (2002; 2011; 2014), Comin-Chiaramonti and Gomes (2005), Gibson et al. (2006), Gomes et al. (2011) and references therein. Deccan data are from Simonetti et al. (1998) and Sen et al. (2009); alkaline rocks locally interbedded within CFB (e.g., Melluso et al., 1995) are not considered. Karoo data are from Harmer et al. (1998) and de Bruiyn et al. (2005).

Figure 7 – Chondrite-normalized Rare Earth Element (REE) and Primitive Mantle-normalized incompatible element patterns for mafic rocks from alkaline-carbonatite complexes coeval with CFB from a) Paranà-Etendeka, b) Deccan and c) Karoo igneous provinces. Paranà-Etendeka data are from Beccaluva et al. (1992; 2017); Coltorti et al. (1993); Trumbull et al. (2003), Comin-Chiaramonti et al. (2002; 2011; 2014); Comin-Chiaramonti and Gomes (2005); Gibson et al. (2006); Gomes et al. (2011) and references therein. Deccan data are from Sen et al. (2009), whereas Karoo data are from Harmer et al. (1998) and de Bruiyn et al. (2005). Normalizing factors after Sun and McDonough (1989).

Figure 8 – Incompatible element distribution of alkaline basic melts coeval with CFB in the Paranà-Etendeka province. a) modelling indicates that Etendeka alkaline basic melts could be generated

either by 2% or 10% batch melting of a PM source hybridized with 20% and 40% amphibole-rich metasomatic veins, respectively. Composition of metasomatic veins, mineral modes and melting coefficients are after Pilet et al. (2011). b) Modelling for Brazilian alkaline basic magmas requires the significant presence of phlogopite (in addition to amphibole) in the source. Best fit is obtained either by 2% or 8% batch melting of a PM source hybridized with 40% and 90% of metasomatic veins, respectively. In this case, amphibole-rich metasomatic veins (Pilet et al., 2011) contain up to 30% of phlogopite. Data source as in Fig. 7. Partition coefficients (*Kd*) from the GERM database. Normalizing factors are from Sun and McDonough (1989).

Figure 9 – (a) Sr-Nd and (b) Pb isotopic composition of CFB and coeval alkaline-carbonatite complexes for the Paranà-Etendeka igneous province. Data from GEOROC and from Huang et al. (1995); Milner and Le Roex (1996); Le Roex and Lanyon (1998); Harris et al., (1999); Alberti et al. (1999); Trumbull et al. (2003; 2007); Comin-Chiaramonti et al. (2007; 2011); Gomes et al. (2011); Beccaluva et al. (2017); Owen-Smith et al. (2017). Isotopic composition of Gough and Tristan hot spot tracks are from Hoernle et al. (2015). Reference mantle end-members (DM, EM1, EM2, HIMU and FOZO) are also reported for comparison (Zindler and Hart, 1986; Hofmann, 1997; Stracke, 2012). Sr-Nd initial isotopic values have been calculated at 132 Ma.

Figure 10 – Paleogeographic reconstruction of the Deccan igneous province at ca. 65 Ma reporting the spatial distribution of HT1 and LT suites (modified after Natali et al., 2017 and references therein). Note that the centre of the encircled equidimensional area (Reunion hot spot) corresponds to the distribution of HT1 picrite-basalt, the maximum concentration of nearly coeval alkaline (-carbonatite) complexes and the intersection of the main rift structures.

Figure 11 – (a) Sr-Nd and (b) Pb isotopic composition of CFB and coeval alkaline-carbonatite complexes for the Deccan igneous province. Data from GEOROC and from Simonetti et al. (1995;

1998) and Sen et al. (2009). Reference mantle end-members (DM, EM1, EM2, HIMU and FOZO) are also reported for comparison (Zindler and Hart, 1986; Hofmann, 1997; Stracke, 2012). Sr-Nd initial isotopic values have been calculated at 65 Ma.

Figure 12 –Paleogeographic reconstruction of the Karoo igneous province at ca. 170 Ma, reporting the spatial distribution of HT2, HT1 and LT suites (modified after Natali et al., 2017 and references therein). Note that the central CFB area correspond to a triple junction defined by the convergence of dike swarms, the distribution of HT2 picrite-basalt and the location of nearly coeval alkaline-carbonatite complexes.

Figure 13 – (a) Sr-Nd and (b) Pb isotopic composition of CFB and coeval alkaline-carbonatite complexes for the Karoo igneous province. Data from GEOROC and from Hawkesworth et al. (1984) and Harmer et al. (1998). Reference mantle end-members (DM, EM1, EM2, HIMU and FOZO) are also reported for comparison (Zindler and Hart, 1986; Hofmann, 1997; Stracke, 2012). Sr-Nd initial isotopic values have been calculated at 180 Ma.

Figure 14 – Impinging of the mantle plume head on the pre-existing lithosphere caused a dramatic thermal anomaly (T_{ex} 250-300°C) coupled with bulging, thinning and development of extensional lineaments that intersected and radiated from the plume axial zone. The combined tectonic and thermal effects at the plume axis could explain the contemporaneous generation, virtually on the same plumbing system, of high-MgO CFB and alkaline magmas from the convective asthenosphere and the overlying lithosphere, respectively, under distinct P-T-X conditions (see inset): 1) high-MgO CFB could derive from volatile-poor sublithospheric mantle sources where the solidus is crossed at T_p 1500-1600°C, 4-5 GPa by moderate-high melting degree under nearly-adiabatic conditions; 2) parental melts of the alkaline-carbonatite complexes formed by a generally low degree of melting in the lower portion of the lithosphere (T_p 1300-1400°C, P 2-3 GPa), where the

solidus is variably depressed owing to the common occurrence of hydrated and carbonated components. Data for volatile-rich (hydrated and carbonated lherzolite) and volatile-poor (anhydrous lherzolite) solidi are taken from the literature (Turner et al., 1996; Walter, 1998; Thompson et al., 2001; Green and Fallon, 2005; Gudfinnsson and Presnall, 2005). The thermal regime and composition of the lithosphere is based on mantle xenoliths from the Gondwana realm that consist of Sp- to Gt-lherzolite/harzburgite variably enriched by metasomatic phases (amphibole, phlogopite and carbonates; Rivalenti et al., 2000; Fodor et al., 2002; Dessai et al., 2004; Griffin et al., 2003; Beccaluva et al., 2007; 2008; 2011; Karmalkar et al., 2009; Natali et al., 2013; Bianchini et al., 2014; Sgualdo et al., 2015; Stanley et al., 2015). The hatched area corresponds to the asthenosphere-lithosphere transition.

Table captions:

Supplementary Table 1 – Major element composition of calculated primary melts for representative high-MgO CFB and coeval alkaline basic melts Paranà-Etendeka, Deccan Karoo LIPs. Reconstruction of CFB primary melts has been obtained by the Herzberg and Asimow (2015) model assuming a mantle source with mg# 0.90, whereas alkaline primary melt have been obtained using the Putirka (2016) model assuming mg# 0.87 for the metasomatized source. Thermobarometric estimates have been obtained using the models of Guddfinnsonn and Presnall (2005), Herzberg et al. (2007), Lee et al., (2009), Herzberg and Asimow (2015), Putirka (2016) for CFB, whereas for alkaline magmas only the Putirka (2016) model could be applied.

Paragraphs at lines 90-126, 127-192 and 310-342 have been broken up.

The problem with horizontal axis of Fig. 3 has been fixed.

Arial font has been used for labels in Fig. 4.

The problem with vertical axis of Fig. 7a has been fixed.

Acronyms of mantle end-members in the isotopic diagrams of Figs. 9, 11 and 13 have been homogeneised.

Figure 1

Click here to download high resolution image

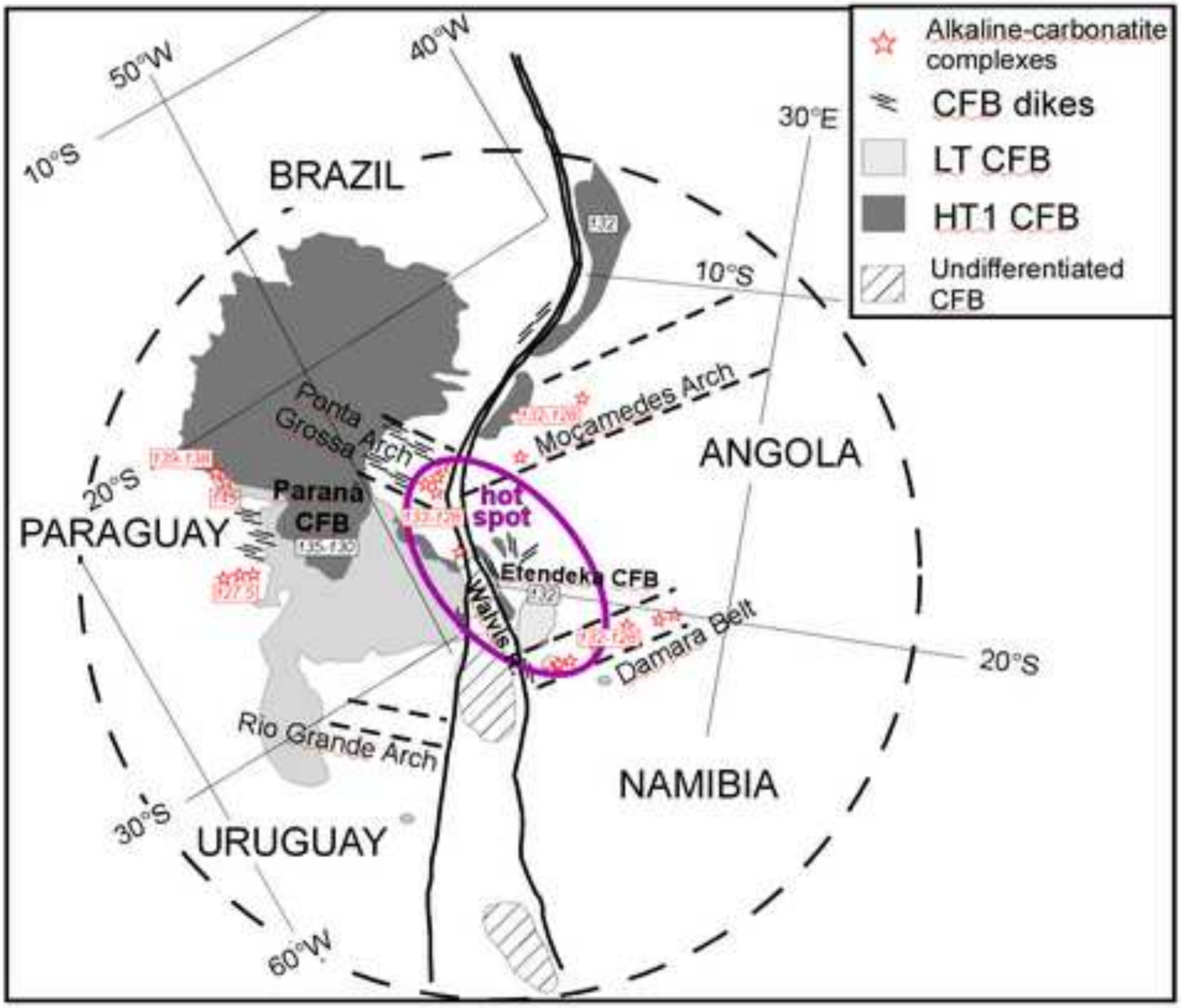

Figure 2

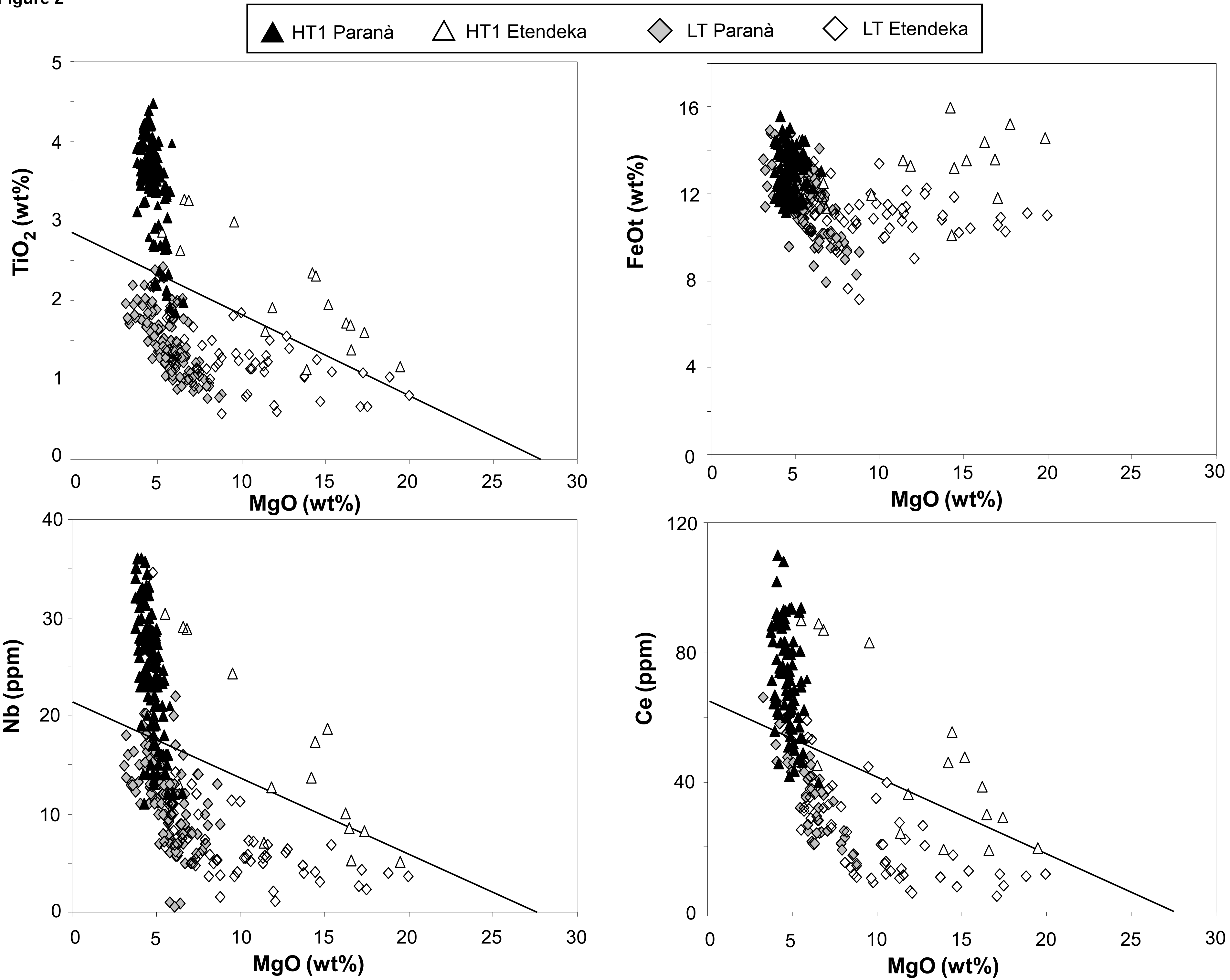
HT1 Paranà
HT1 Etendeka
LT Paranà
LT Etendeka
TiO_2 (wt%)
MgO (wt%)
FeOt (wt%)
MgO (wt%)
Nb (ppm)
MgO (wt%)
Ce (ppm)
MgO (wt%)

Figure 3

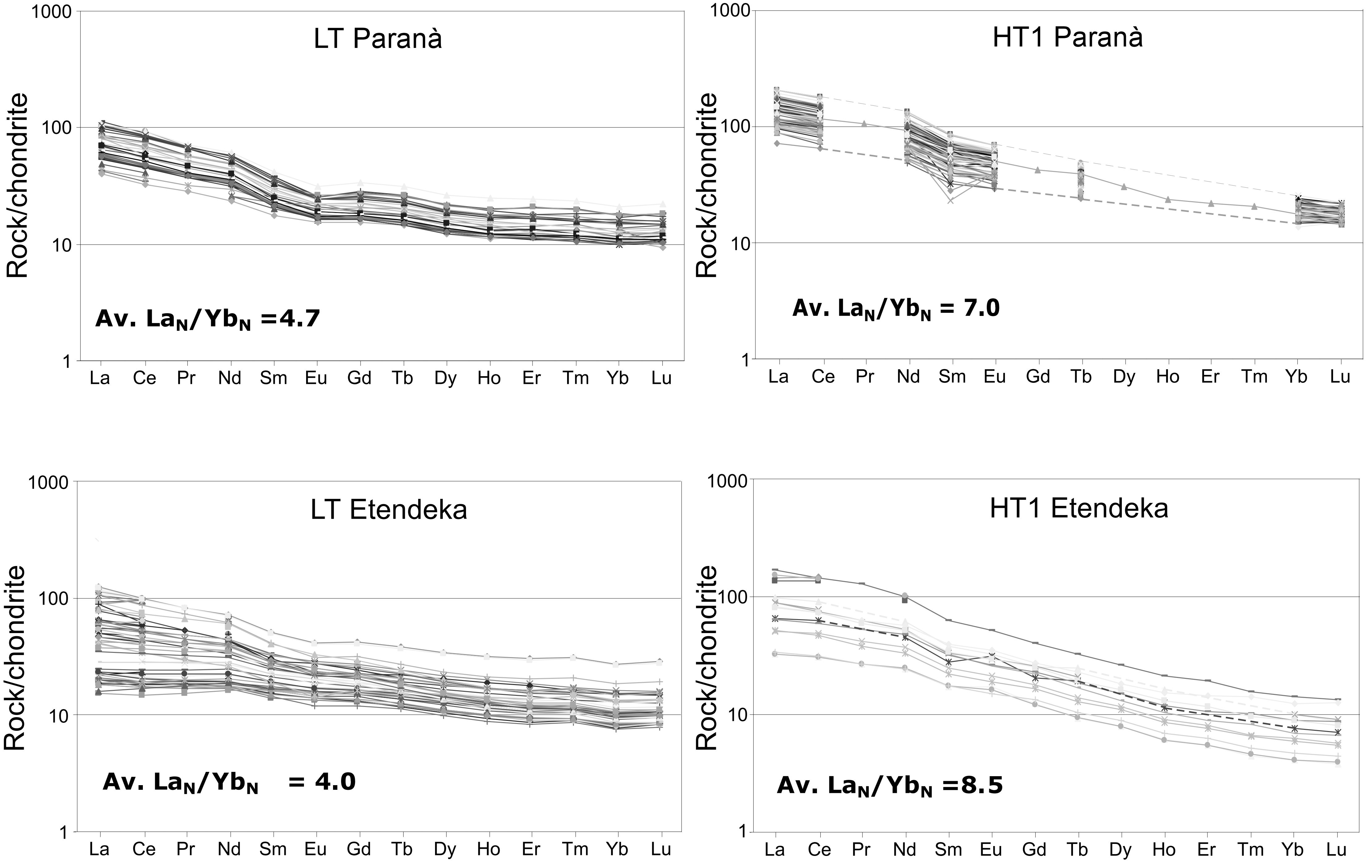

LT Paranà
HT1 Paranà
LT Etendeka
HT1 Etendeka
Rock/chondrite
1000
100
10
1
La Ce Pr Nd Sm Eu Gd Tb Dy Ho Er Tm Yb Lu
Av. La_N/Yb_N =4.7
Av. La_N/Yb_N = 7.0
Av. La_N/Yb_N = 4.0
Av. La_N/Yb_N =8.5

Figure 4

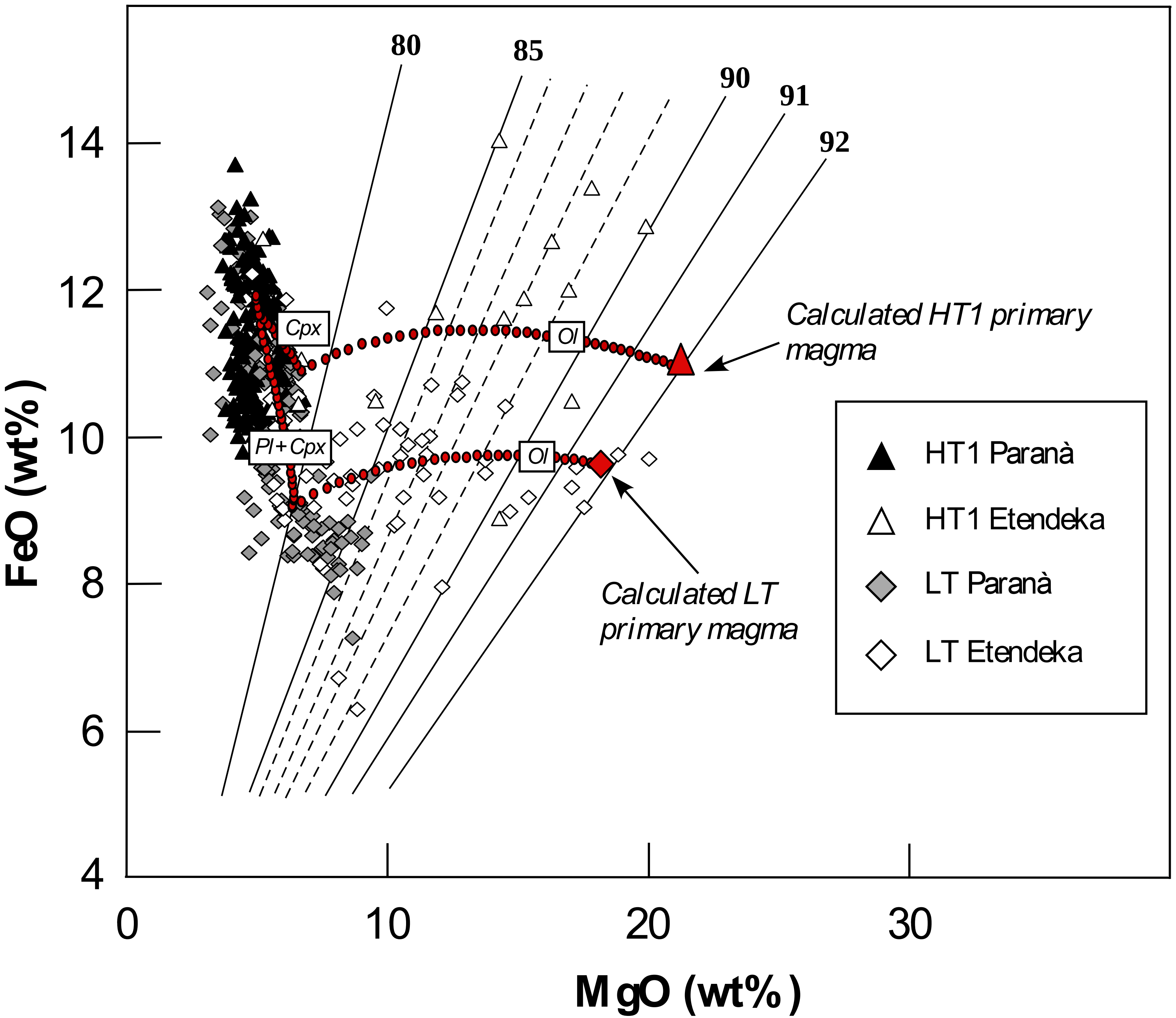

80
85
90
91
92
14
12
10
8
6
4
0
10
20
30
FeO (wt%)
MgO (wt%)
Cpx
Pl+Cpx
Ol
Ol
Calculated HT1 primary magma
Calculated LT primary magma
HT1 Paranà
HT1 Etendeka
LT Paranà
LT Etendeka

Figure 5

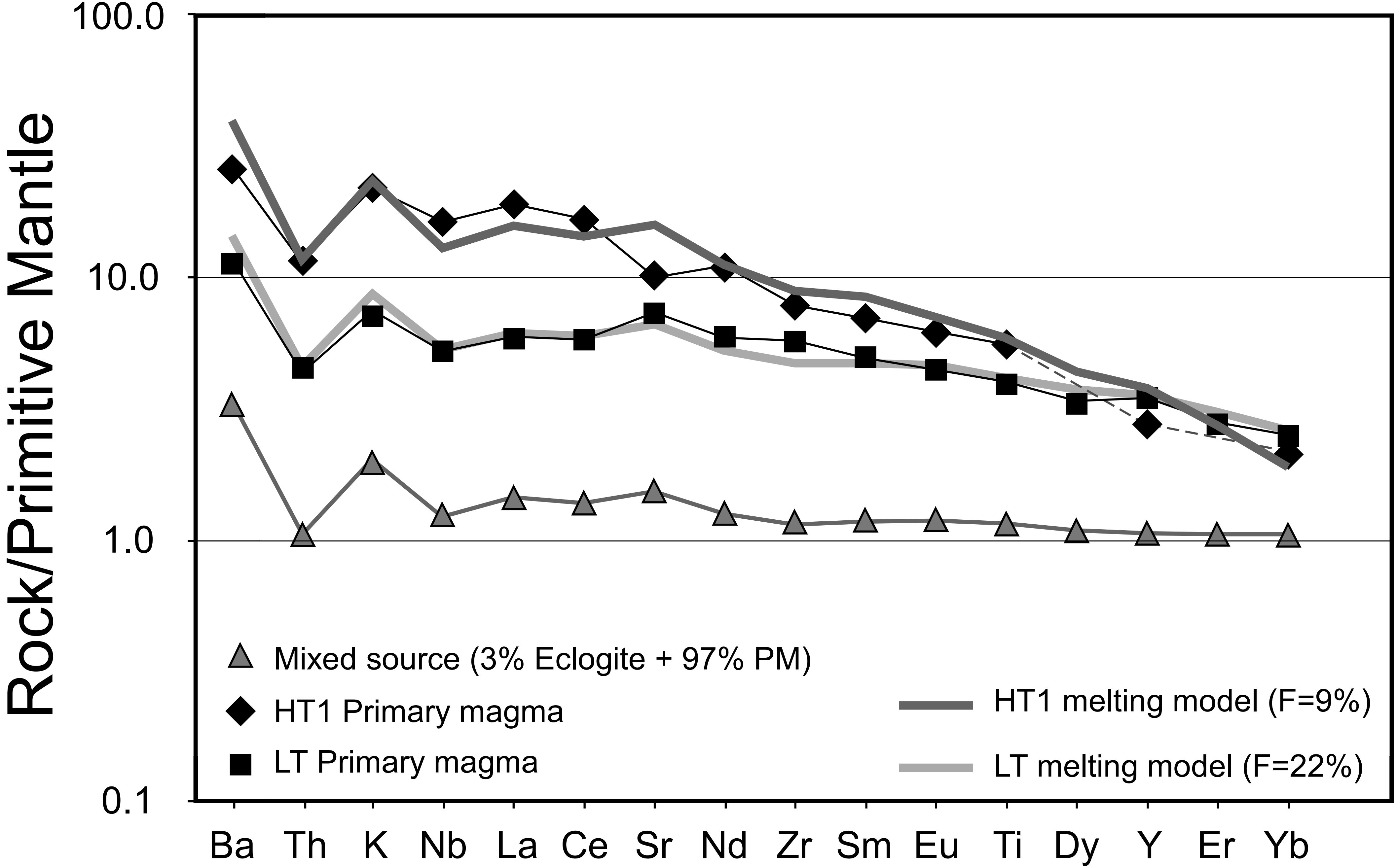
100.0
10.0
1.0
0.1
Rock/Primitive Mantle
Ba
Th
K
Nb
La
Ce
Sr
Nd
Zr
Sm
Eu
Ti
Dy
Y
Er
Yb
Mixed source (3% Eclogite + 97% PM)
HT1 Primary magma
LT Primary magma
HT1 melting model (F=9%)
LT melting model (F=22%)

Figure 6

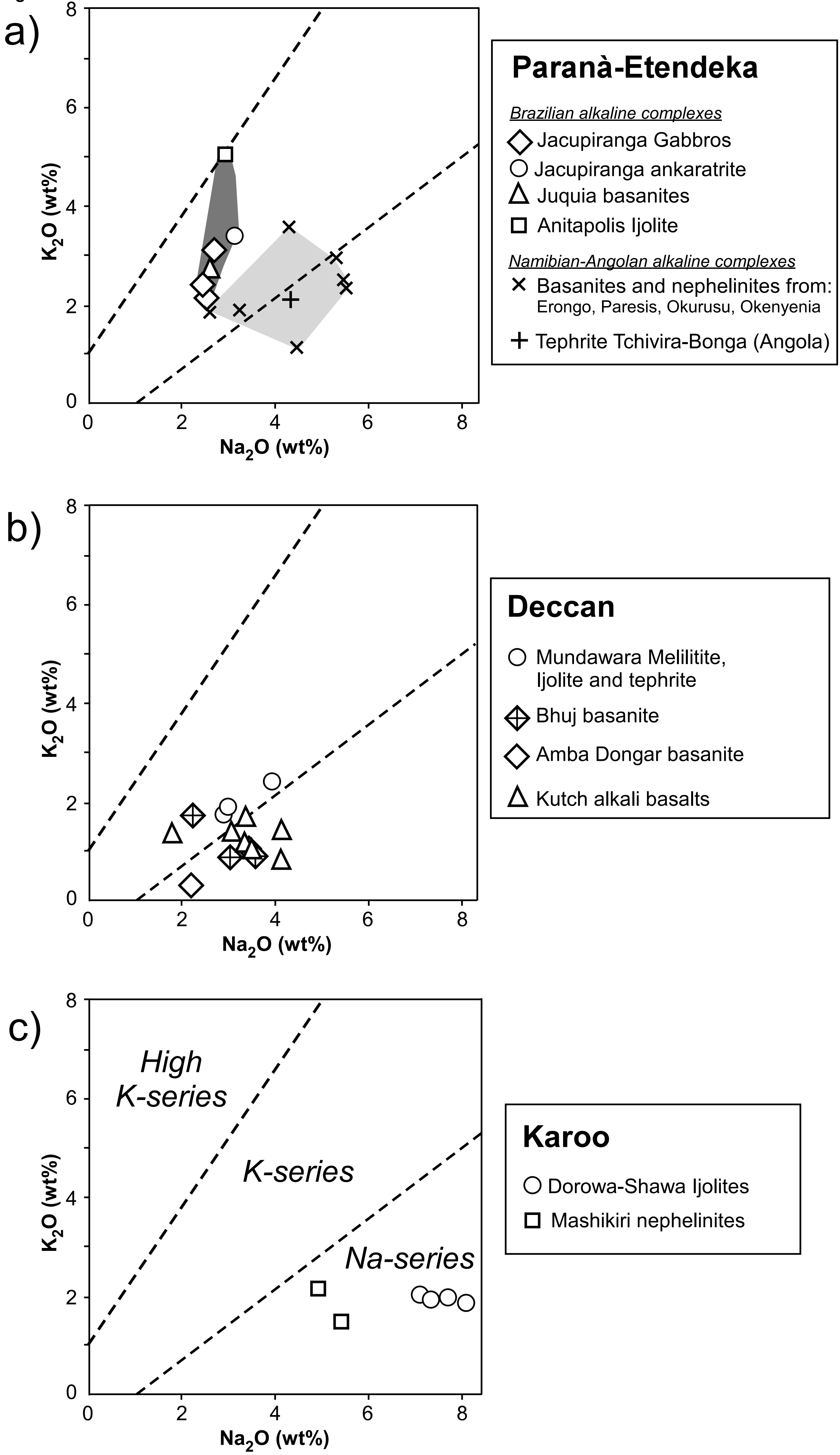

a)
Paranà-Etendeka
Brazilian alkaline complexes
Jacupiranga Gabbros
Jacupiranga ankaratrite
Juquia basanites
Anitapolis Ijolite
Namibian-Angolan alkaline complexes
Basanites and nephelinites from:
Erongo, Paresis, Okurusu, Okenyenia
Tephrite Tchivira-Bonga (Angola)
b)
Deccan
Mundawara Melilitite,
Ijolite and tephrite
Bhuj basanite
Amba Dongar basanite
Kutch alkali basalts
c)
High
K-series
K-series
Na-series
Karoo
Dorowa-Shawa Ijolites
Mashikiri nephelinites
K_2O (wt%)
Na_2O (wt%)
0
2
4
6
8

Figure 7

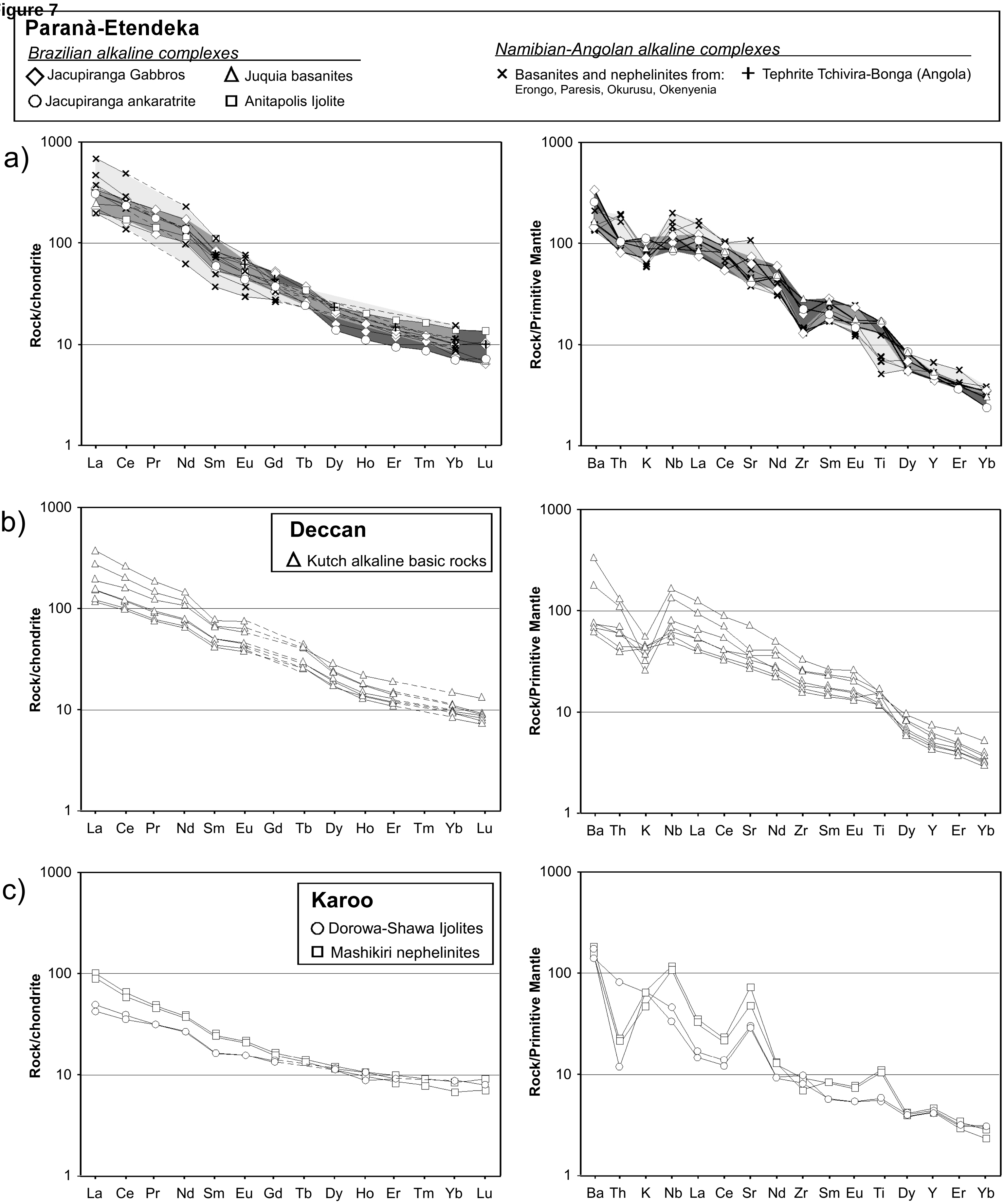

Paranà-Etendeka
Brazilian alkaline complexes
Jacupiranga Gabbros
Juquia basanites
Jacupiranga ankaratrite
Anitapolis Ijolite
Namibian-Angolan alkaline complexes
Basanites and nephelinites from:
Erongo, Paresis, Okurusu, Okenyenia
Tephrite Tchivira-Bonga (Angola)
a)
b)
Deccan
Kutch alkaline basic rocks
c)
Karoo
Dorowa-Shawa Ijolites
Mashikiri nephelinites
Rock/chondrite
Rock/Primitive Mantle
1000
100
10
1
La Ce Pr Nd Sm Eu Gd Tb Dy Ho Er Tm Yb Lu
Ba Th K Nb La Ce Sr Nd Zr Sm Eu Ti Dy Y Er Yb

Figure 8

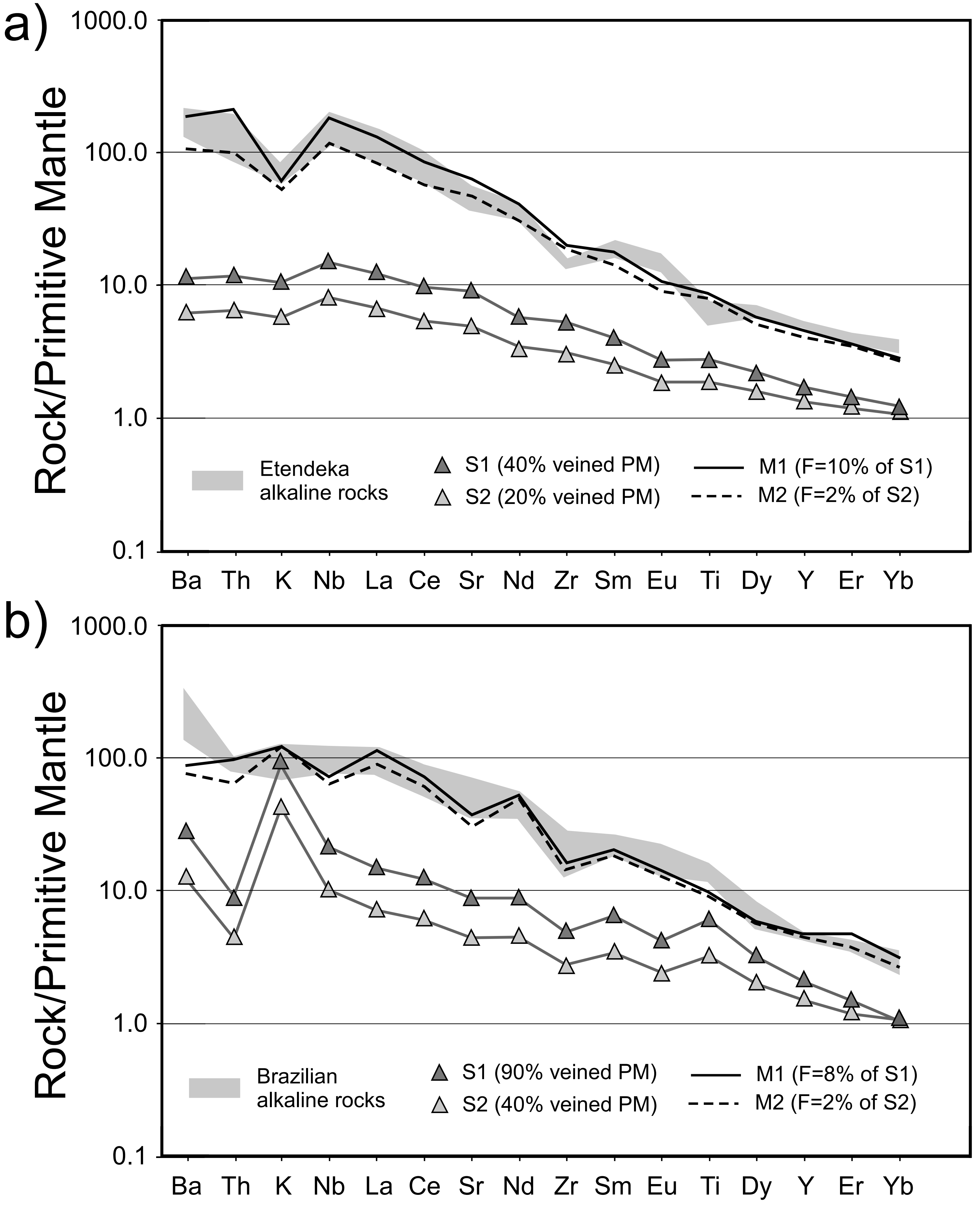

a)
1000.0
100.0
10.0
1.0
0.1
Rock/Primitive Mantle
Etendeka
alkaline rocks
S1 (40% veined PM)
S2 (20% veined PM)
M1 (F=10% of S1)
M2 (F=2% of S2)
Ba Th K Nb La Ce Sr Nd Zr Sm Eu Ti Dy Y Er Yb
b)
1000.0
100.0
10.0
1.0
0.1
Rock/Primitive Mantle
Brazilian
alkaline rocks
S1 (90% veined PM)
S2 (40% veined PM)
M1 (F=8% of S1)
M2 (F=2% of S2)
Ba Th K Nb La Ce Sr Nd Zr Sm Eu Ti Dy Y Er Yb

Figure 9

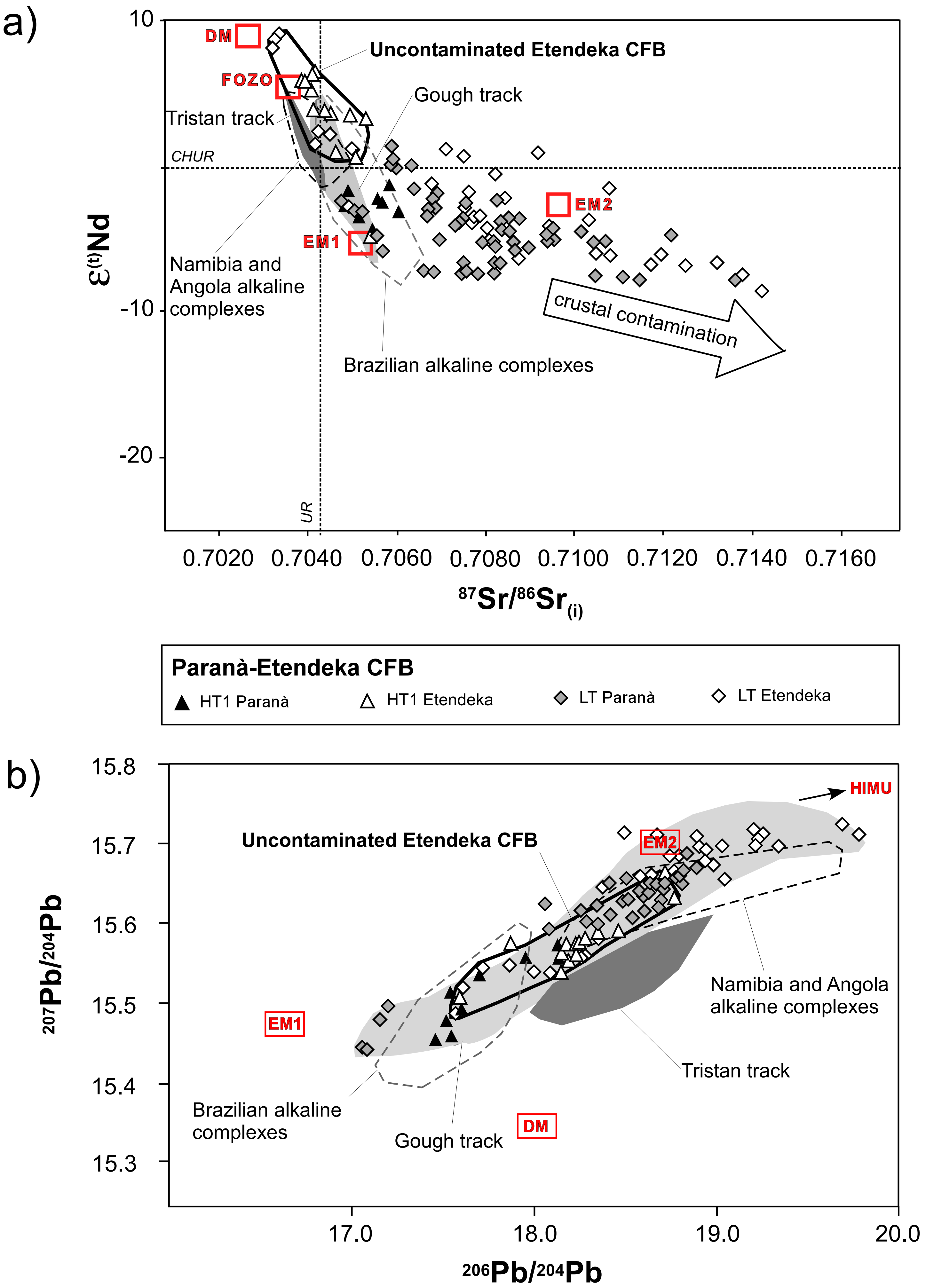

a)
10
-10
-20
DM
FOZO
EM1
EM2
Uncontaminated Etendeka CFB
Gough track
Tristan track
CHUR
UR
Namibia and Angola alkaline complexes
Brazilian alkaline complexes
crustal contamination
ε(t)Nd
0.7020
0.7040
0.7060
0.7080
0.7100
0.7120
0.7140
0.7160
87Sr/86Sr(i)
Paranà-Etendeka CFB
HT1 Paranà
HT1 Etendeka
LT Paranà
LT Etendeka
b)
15.8
15.7
15.6
15.5
15.4
15.3
HIMU
Uncontaminated Etendeka CFB
EM2
EM1
DM
Namibia and Angola alkaline complexes
Tristan track
Brazilian alkaline complexes
Gough track
17.0
18.0
19.0
20.0
206Pb/204Pb
207Pb/204Pb

Figure 10

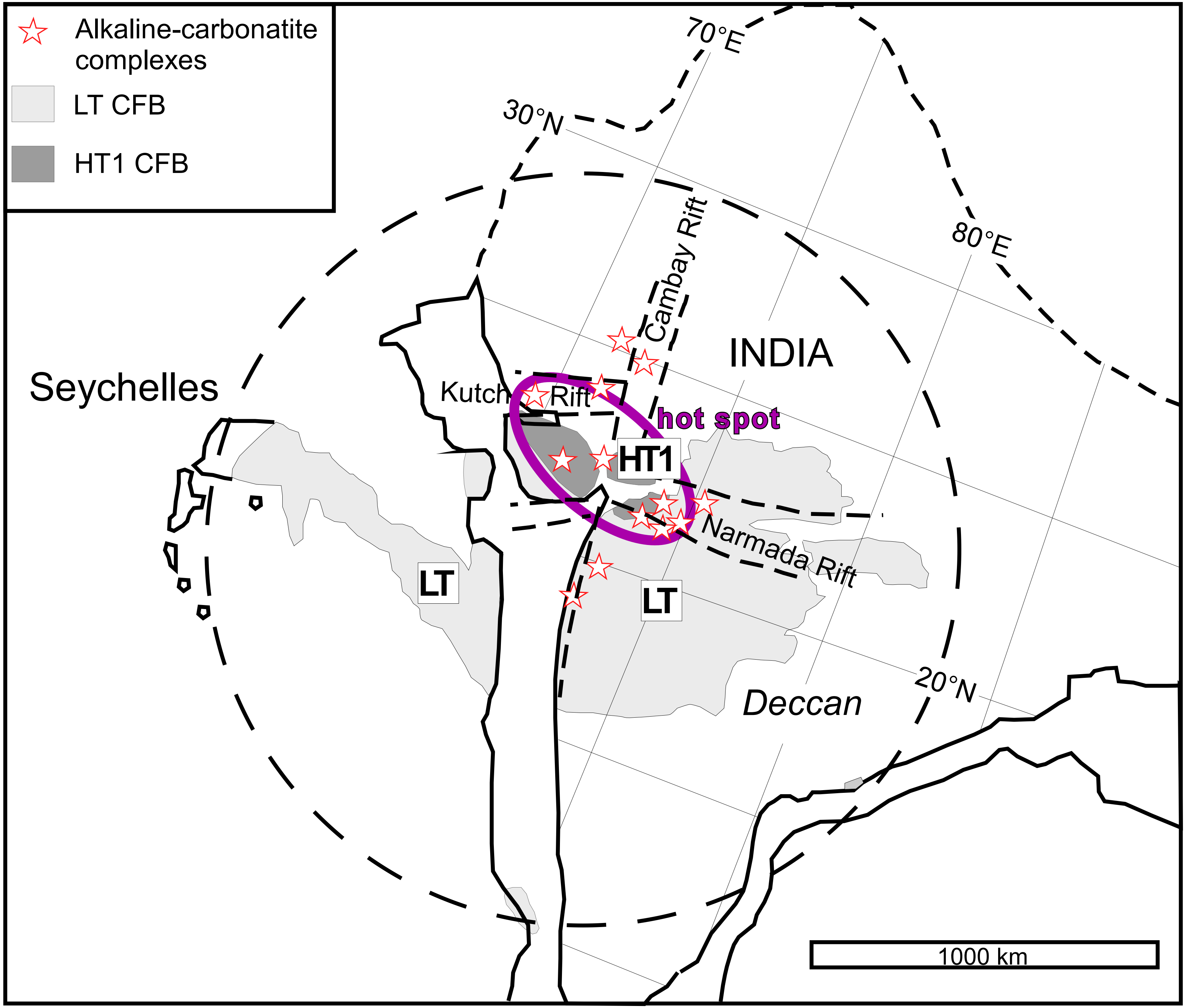

Alkaline-carbonatite complexes
LT CFB
HT1 CFB
70°E
30°N
80°E
20°N
Cambay Rift
INDIA
Seychelles
Kutch
Rift
hot spot
HT1
Narmada Rift
LT
LT
Deccan
1000 km

Figure 11

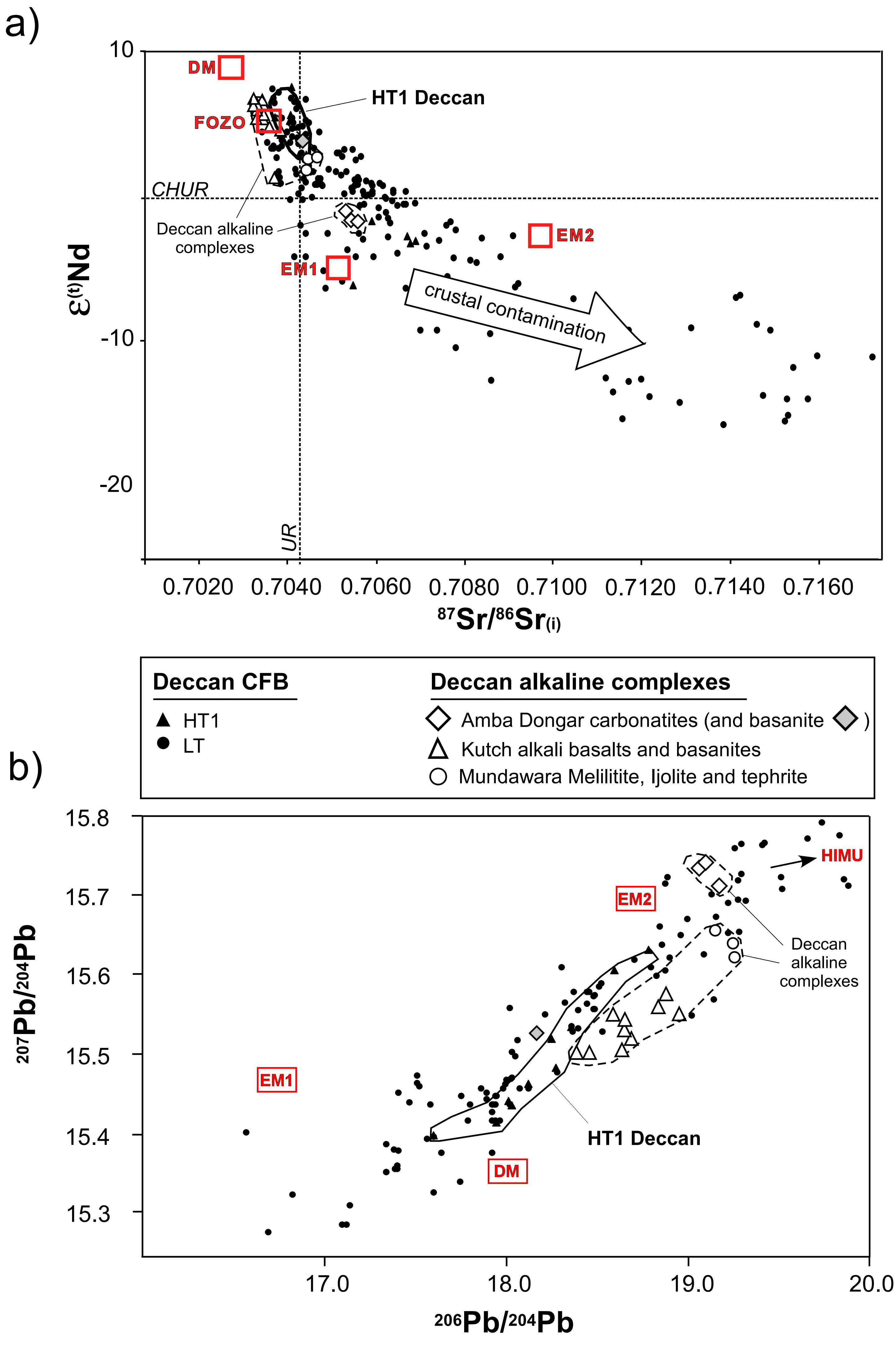

a)
10
-10
-20
DM
FOZO
HT1 Deccan
CHUR
Deccan alkaline
complexes
EM2
EM1
crustal contamination
UR
ε(t)Nd
0.7020
0.7040
0.7060
0.7080
0.7100
0.7120
0.7140
0.7160
87Sr/86Sr(i)
Deccan CFB
HT1
LT
Deccan alkaline complexes
Amba Dongar carbonatites (and basanite)
Kutch alkali basalts and basanites
Mundawara Melilitite, Ijolite and tephrite
b)
15.8
15.7
15.6
15.5
15.4
15.3
HIMU
EM2
Deccan
alkaline
complexes
EM1
HT1 Deccan
DM
207Pb/204Pb
17.0
18.0
19.0
20.0
206Pb/204Pb

Figure 12

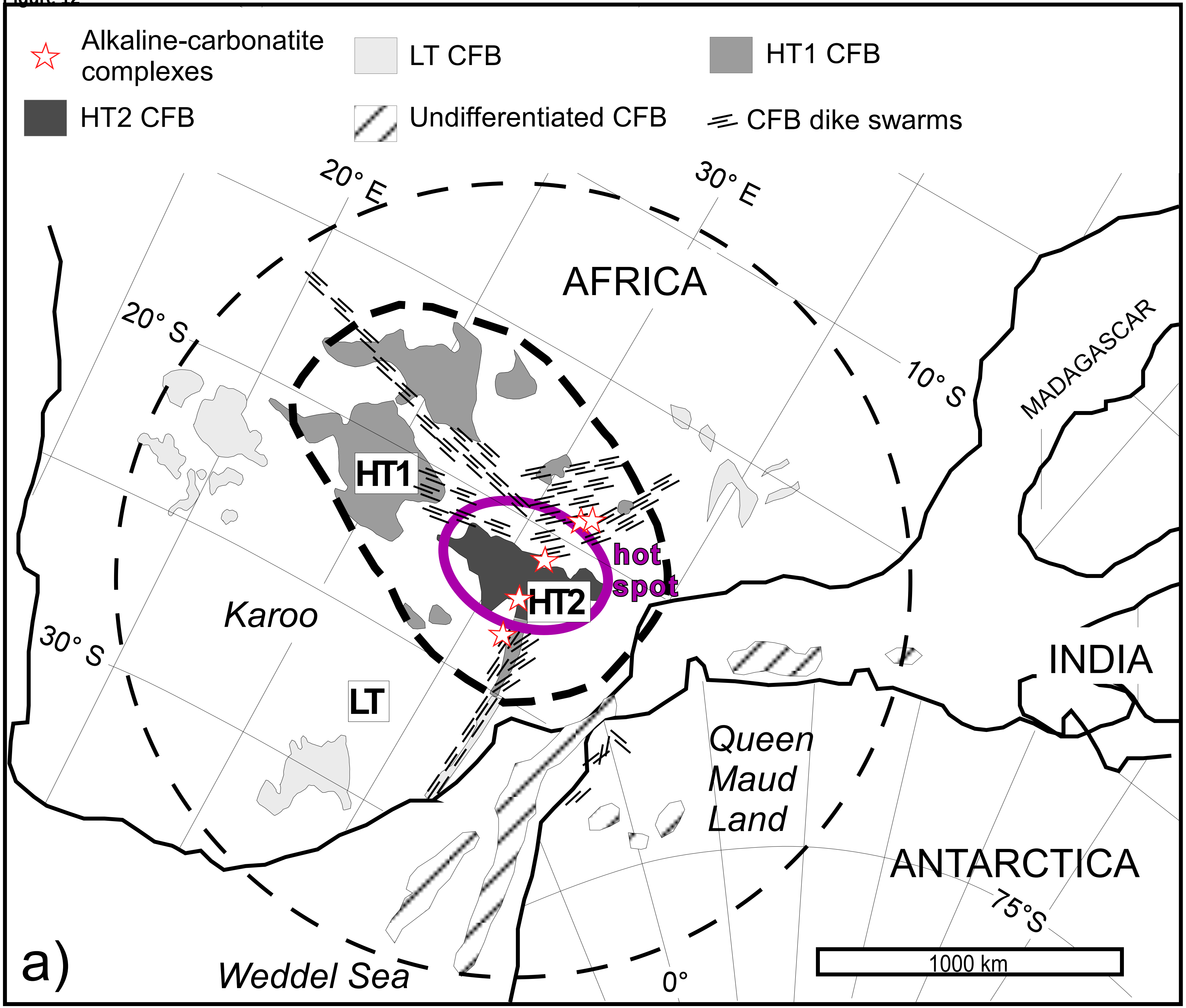
Alkaline-carbonatite complexes
LT CFB
HT1 CFB
HT2 CFB
Undifferentiated CFB
CFB dike swarms
20° E
30° E
AFRICA
20° S
10° S
MADAGASCAR
HT1
hot spot
HT2
Karoo
30° S
LT
INDIA
Queen Maud Land
ANTARCTICA
75°S
1000 km
a)
Weddel Sea
0°

Figure 13

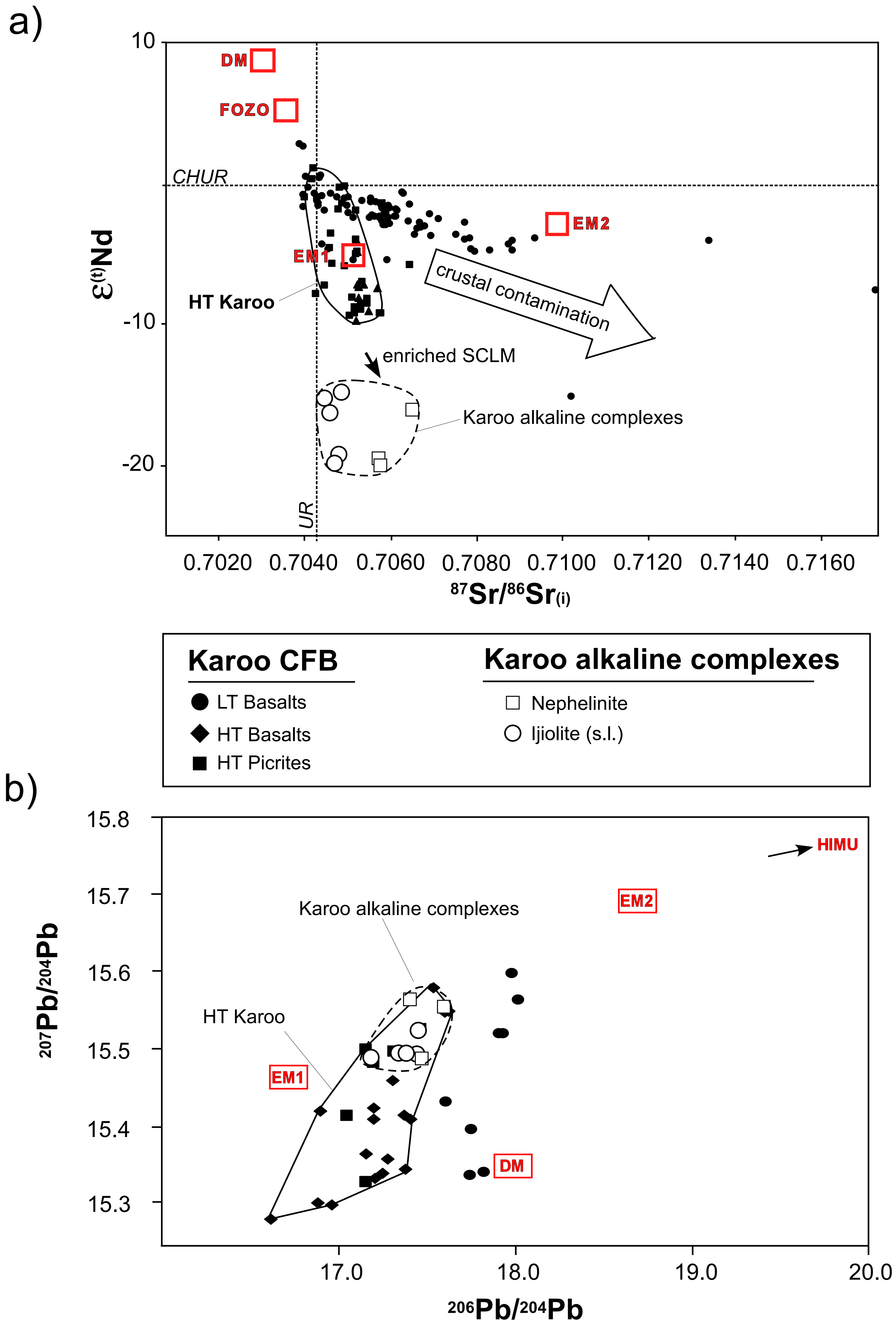

a)
DM
FOZO
CHUR
EM2
EM1
HT Karoo
crustal contamination
enriched SCLM
Karoo alkaline complexes
UR
10
-10
-20
0.7020
0.7040
0.7060
0.7080
0.7100
0.7120
0.7140
0.7160
ε(t)Nd
87Sr/86Sr(i)
Karoo CFB
LT Basalts
HT Basalts
HT Picrites
Karoo alkaline complexes
Nephelinite
Ijiolite (s.l.)
b)
HIMU
EM2
Karoo alkaline complexes
HT Karoo
EM1
DM
15.8
15.7
15.6
15.5
15.4
15.3
17.0
18.0
19.0
20.0
207Pb/204Pb
206Pb/204Pb

Figure 14
Click here to download high resolution image

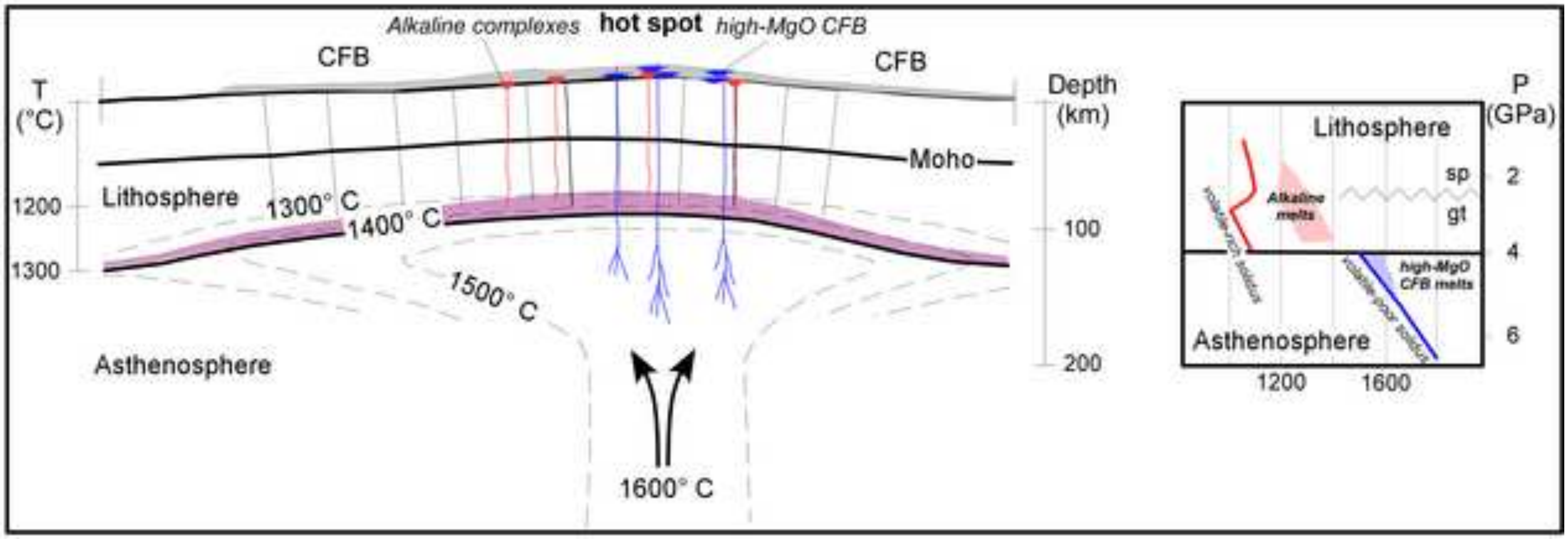

Supplementary Table 1

Click here to download Background dataset for online publication only: Supplementary Table 1_rev2.xls